



Role of and evidence for off-diagonal particle & toroidal momentum transport: experiments, theory & modelling

Clemente Angioni

**With special thanks to
Y. Camenen, F.J. Casson, E. Fable, R.M. McDermott,
A.G. Peeters, J.E. Rice**

On the interest of combining particle and momentum transport



- Particle (& impurity) transport often treated as separate topic, with little (no) connection to other (more noble) transport channels
- Momentum transport often thought to be mainly associated with ion heat transport, due to the limited variation of the Prandtl number around unity

On the interest of combining particle and momentum transport



- Particle (& impurity) transport often treated as separate topic, with little (no) connection to other (more noble) transport channels
- Momentum transport often thought to be mainly associated with ion heat transport, due to the limited variation of the Prandtl number around unity
- Let me say that this is the past
- Today, the problem of transport in tokamak plasmas has to be approached in its entirety, taking into account the strong mutual interactions between all the transport channels (moments of the same distribution function, transport is a non-diagonal matrix ...)
- Under very many aspects, particle and momentum transport are certainly very good friends ...

Outline

- A pragmatic approach, general expressions of particle and toroidal momentum fluxes, similarities and differences
- Main implications on the phenomenology, key observations, back implications on theory
- One step further, deeper in physical understanding
- Nature of different off-diagonal mechanisms, experimental evidences, main parametric dependences, open questions
 - Particle (& impurity) transport
 - Toroidal momentum transport
- Impact of different turbulent regimes on non-diffusive particle and momentum transport (similarities & differences), relevance in the core (and at the edge)

Outline

- **A pragmatic approach, general expressions of particle and toroidal momentum fluxes, similarities and differences**
- **Main implications on the phenomenology, key observations, back implications on theory**
- One step further, deeper in physical understanding
- Nature of different off-diagonal mechanisms, experimental evidences, main parametric dependences, open questions
 - Particle (& impurity) transport
 - Toroidal momentum transport
- Impact of different turbulent regimes on non-diffusive particle and momentum transport (similarities & differences), relevance in the core (and at the edge)

Particle and toroidal momentum fluxes

➤ General simple expressions of radial fluxes

Particle

$$\Gamma_n = n \left(-D_n \frac{\partial \ln n}{\partial r} + V_n \right)$$

Toroidal momentum

$$\Pi_\phi = nmR \left(-\chi_\phi \frac{\partial U_\phi}{\partial r} + V_\phi U_\phi \right) + \Pi_{RS}$$

- Both involve off-diagonal terms, but have important differences
- Density is a positive scalar, toroidal rotation velocity is a component of a vector
- Particle flux involves ONLY off-diagonal terms which are proportional to density
- Momentum flux has additional terms which are NOT proportional to the toroidal velocity (present also when the toroidal velocity and its gradient are zero)
- Diagonal (diffusive) terms: log. density gradient, linear toroidal velocity gradient

Direct implications on the phenomenology, density peaking

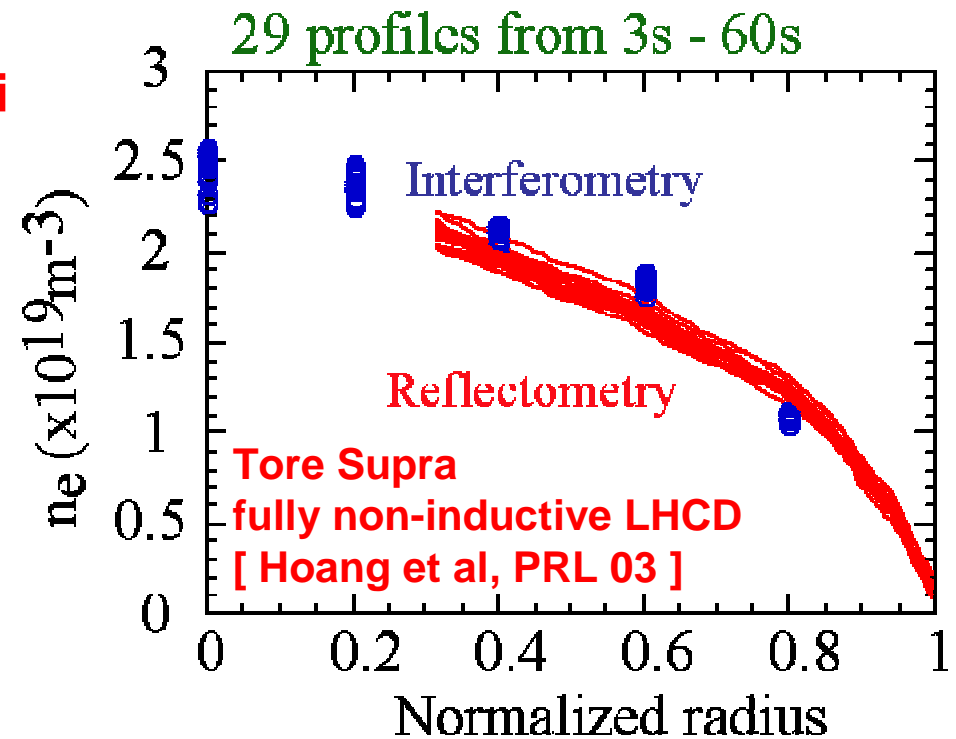


- A density profile can remain centrally peaked also in the absence of a particle source
- Main source of peaking is of non-collisional (turbulent) nature [Coppi PRL 78, Coppi & Sharky NF 1981]

$$\Gamma = -D \nabla n_e + n_e V$$

↓

$$-\frac{\nabla n_e}{n_e} = -\frac{V}{D} + \frac{\Gamma}{n_e D}$$

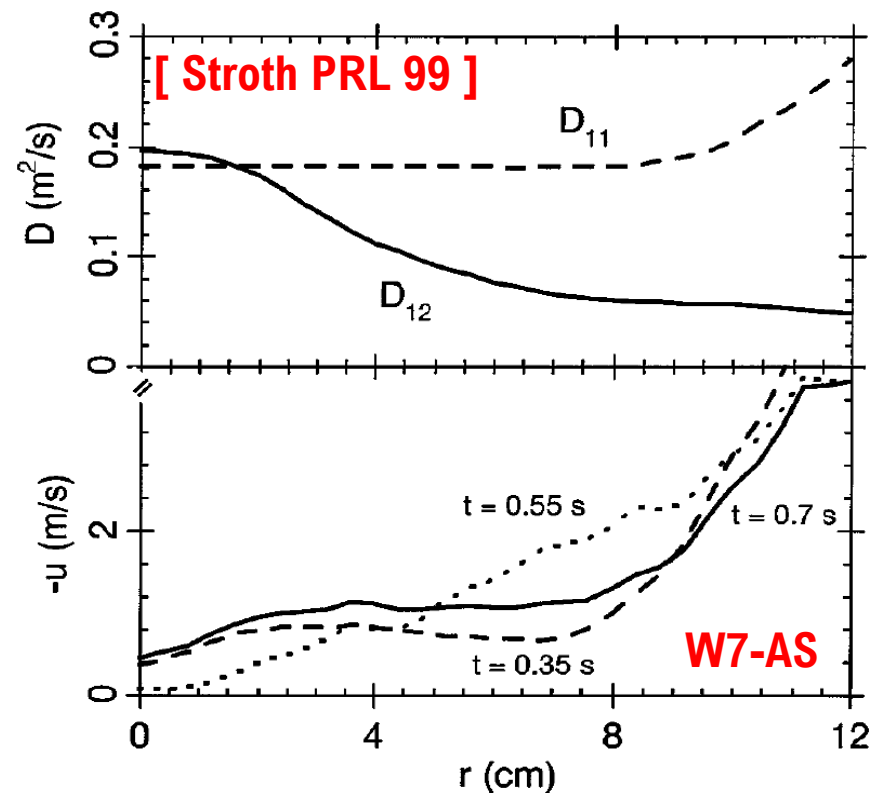
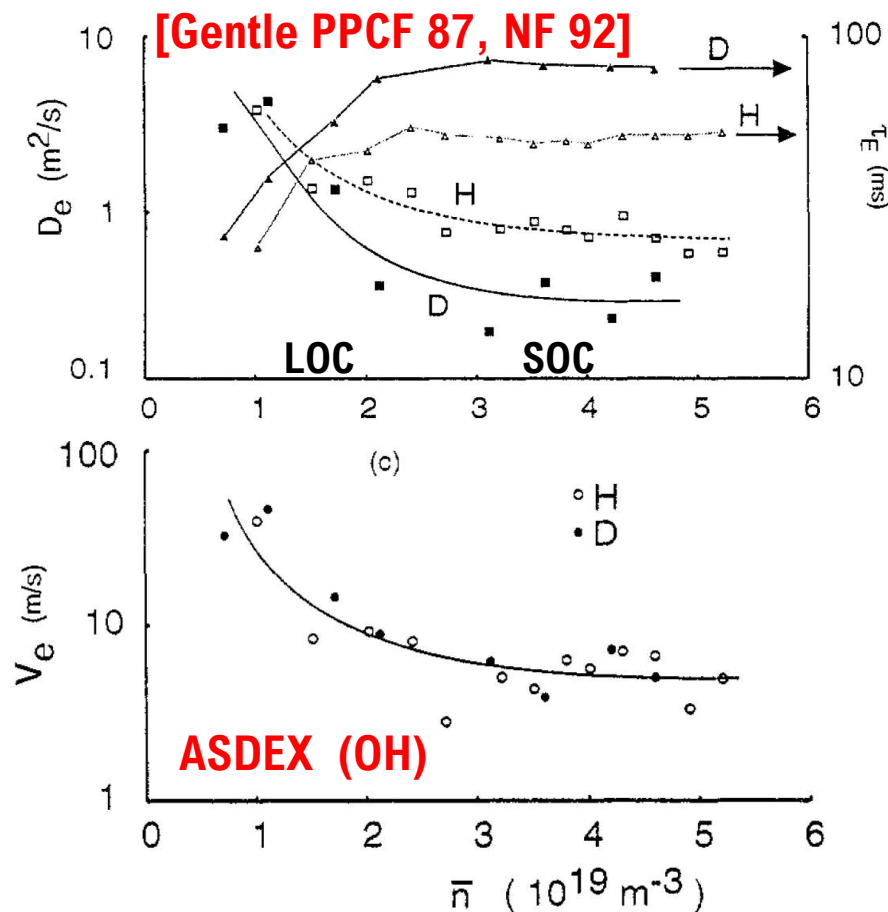


- The existence of a particle convection has been demonstrated by transient transport experiments

Direct implications on the phenomenology, existence of inward particle convection



- The existence of a particle convection has been demonstrated by transient transport experiments (density modulation experiments, gas puff, pellets)



- Pinch particularly large at the edge

Direct implications on the phenomenology, toroidal rotation



- **Transient behaviour of measured rotation profiles cannot be reproduced with a simple diffusive model (existence of off-diagonal terms)**
- **A toroidal rotation profile which is not zero (not flat) can be present in the absence of any externally applied torque (when the torque is only at the edge)**
- **To keep the toroidal rotation profile flat and at zero, a torque has to be applied (existence of residual stress)**
- **The toroidal rotation profile can assume whatever shape, and also cross zero along the minor radius (existence of residual stress)**

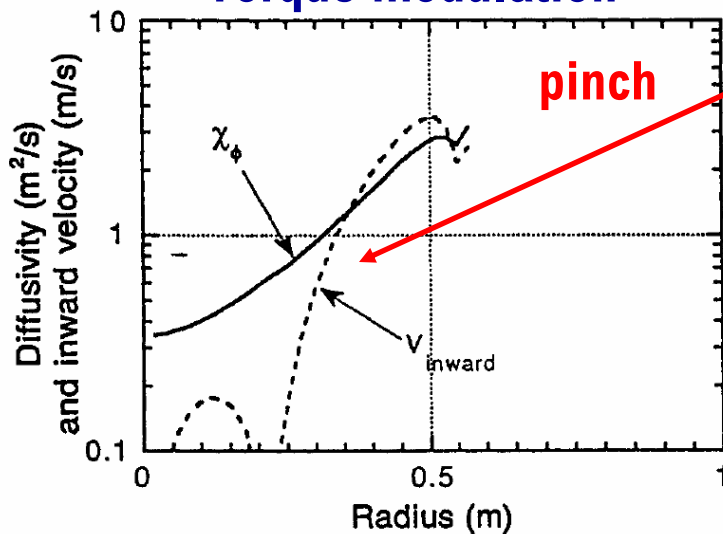
First experimental evidence of existence of off-diagonal term in momentum flux



- Transient behaviour of measured rotation profiles cannot be reproduced with a simple diffusive model (existence of non-diffusive terms)

Nagashima NF 94 at JT-60U

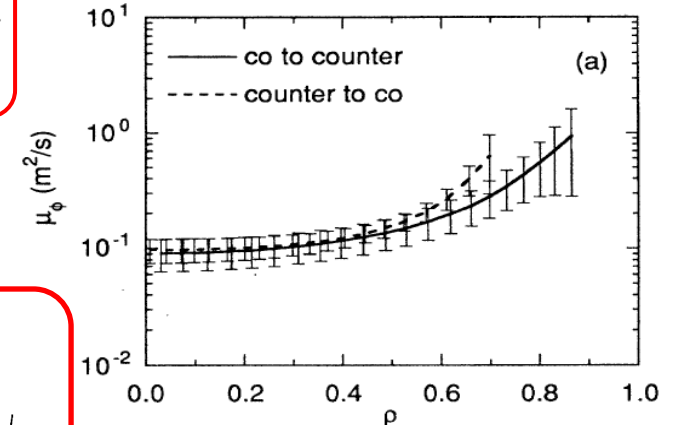
Torque modulation



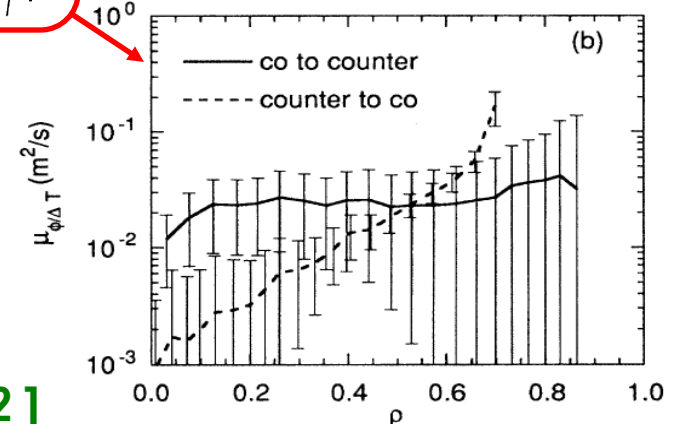
$$M = -mn\chi_\phi \frac{\partial V}{\partial r} - mnv_{\text{inward}}V$$

$$\Gamma_M = \mu_\phi \frac{\partial(m_i n_i v_\phi)}{\partial r} + \mu_{\phi/\Delta T} (v_{th}/T_i) \frac{\partial(m_i n_i T_i)}{\partial r}$$

Ida PRL 95 at JFT-2M
Co- to counter- beams



Residual stress



- Recently confirmed and extended by several studies on existence and dependences of pinch

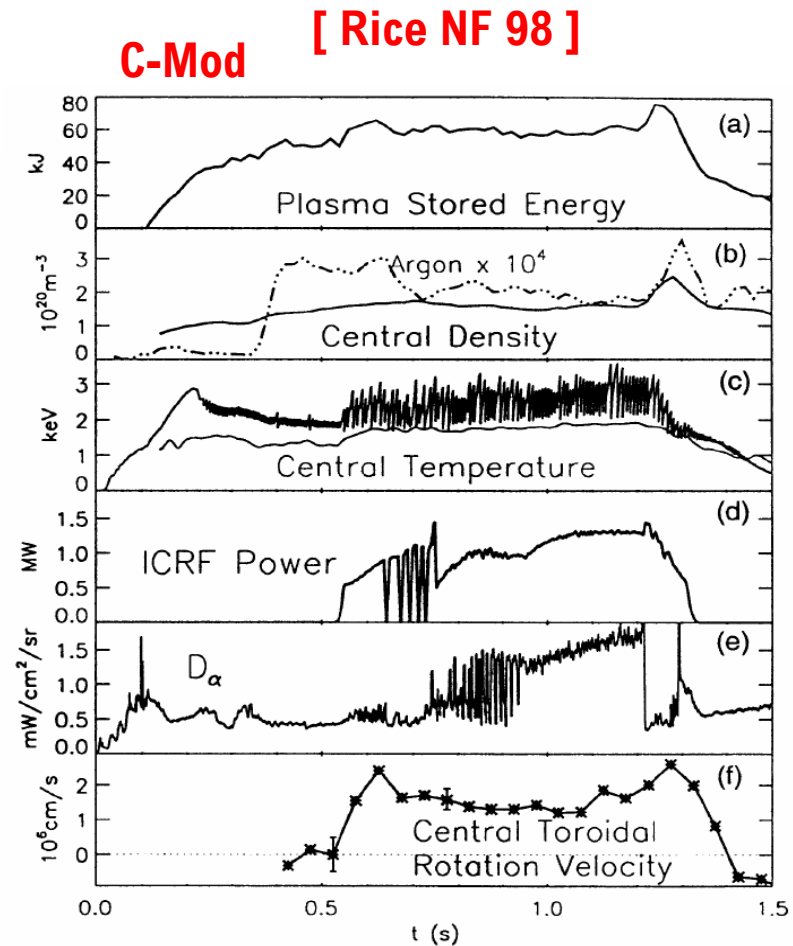
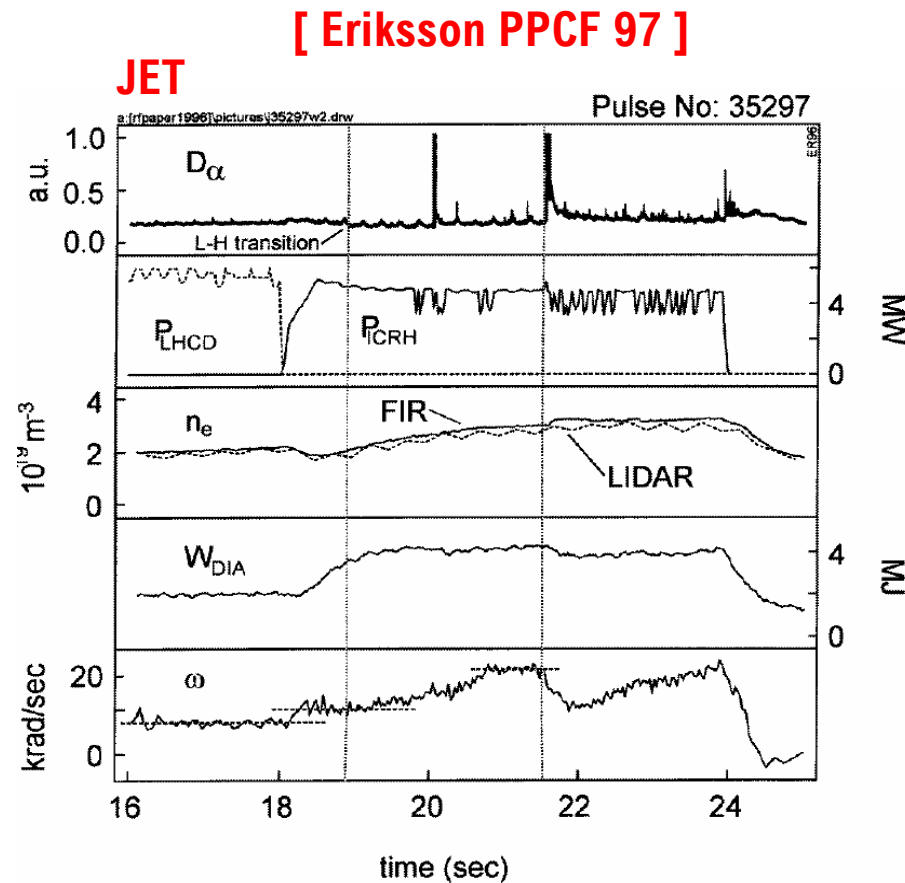
[Yoshida NF 07, Solomon PRL 08,
Tala PRL 09, Kaye NF 09, Solomon NF 09, ...]

Attempts of multi-device comparisons [Yoshida NF 2012]

Direct implications on the phenomenology, intrinsic toroidal rotation



- A toroidal rotation profile which is not zero (not flat) can be present in the absence of any externally applied torque (when the torque is only at the edge)



Direct implications on the phenomenology, existence of residual stress

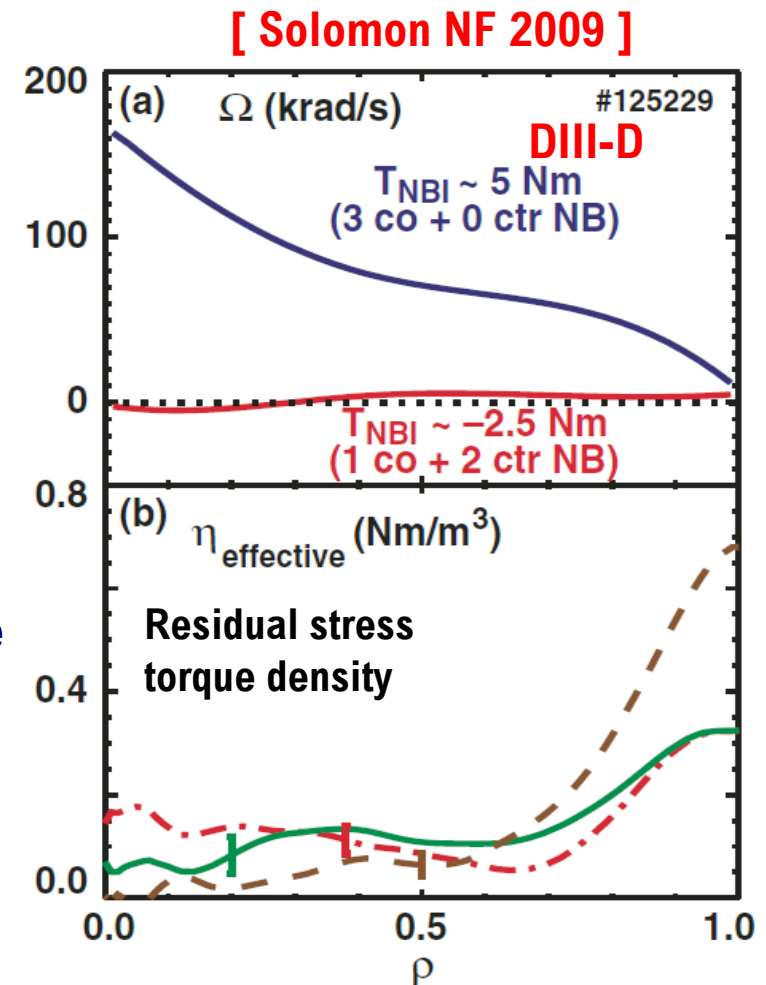


- To keep the toroidal rotation profile flat and at zero, a torque has to be applied (existence of residual stress)

- In this DIII-D experiment, applied torque is counter-current
- Residual stress produces a co-current torque of the size of approx one DIII-D co-current beam source

[Solomon PPCF 08, NF 09]

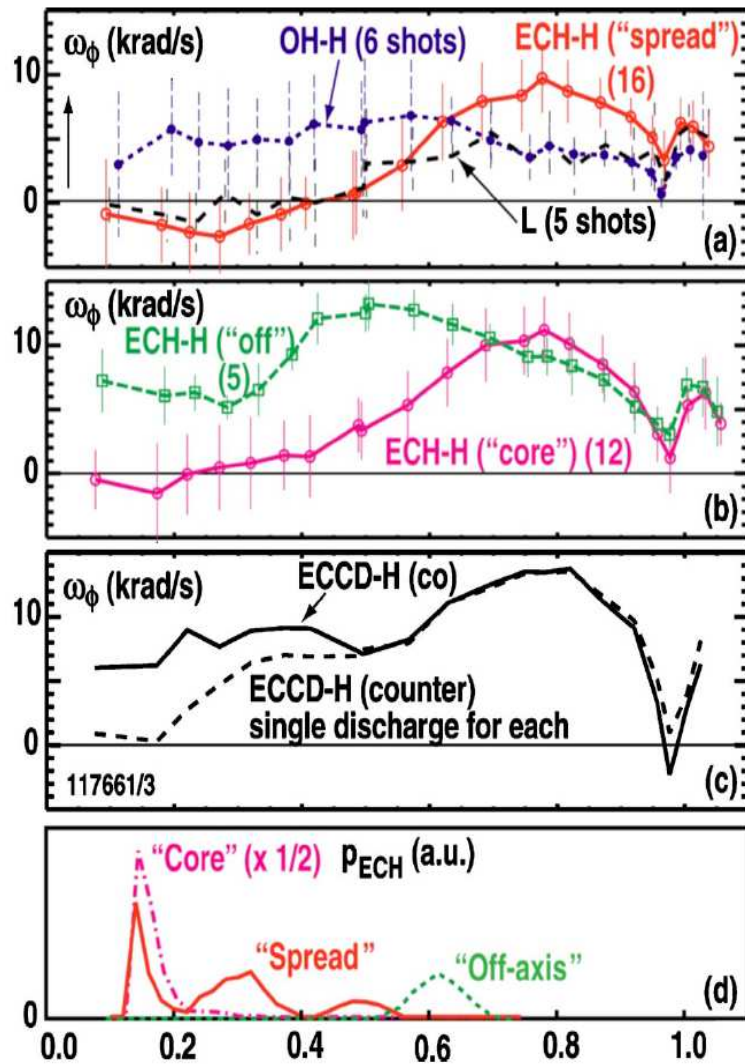
- Effective residual stress torque density profile is larger at the edge
- Sign and magnitude of residual stress in different scenarios is one of the critical questions to answer



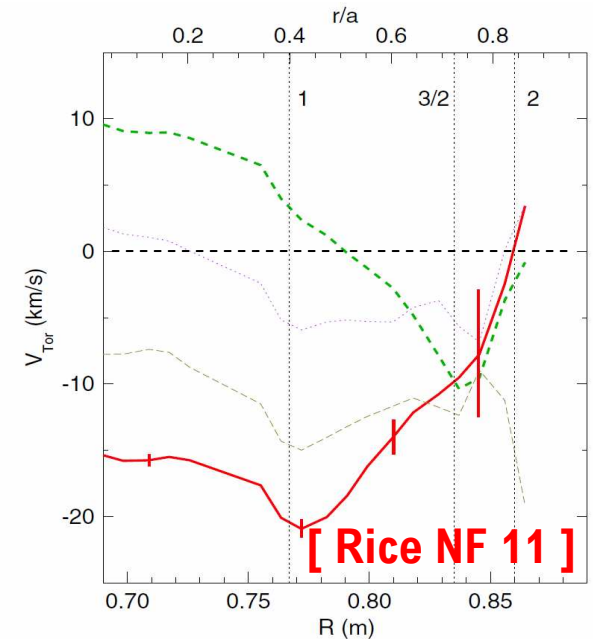
Combination of pinch & residual stress: intrinsic toroidal rotation profile can have whatever shape



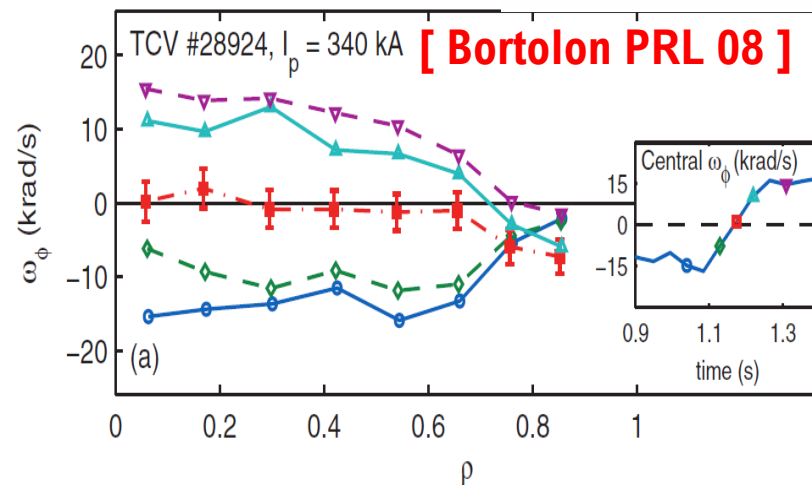
[deGrassie PoP 07]



➤ It can cross zero along the minor radius (existence of residual stress)



[Rice NF 11]



Outline

- A pragmatic approach, general expressions of particle and toroidal momentum fluxes, similarities and differences
- Main implications on the phenomenology, key observations, back implications on theory
- **One step further, deeper in physical understanding**
- **Nature of different off-diagonal mechanisms, experimental evidences, main parametric dependences, open questions**
 - **Particle (& impurity) transport**
 - **Toroidal momentum transport**
- Impact of different turbulent regimes on non-diffusive particle and momentum transport (similarities & differences), relevance in the core (and at the edge)

More subtle differences, decomposing the expressions of the fluxes, particle transport



- A decomposition of the off-diagonal contributions of the fluxes is possible from the RHS of the GK equation (radial gradient of the Maxwellian)
- Particle flux (even velocity moment), off-diagonal terms directly produced by the magnetic geometry and the velocity dependences of the gyro-center drifts

$$\frac{\Gamma_n}{n} = -D_n \frac{1}{n} \frac{\partial n}{\partial r} - D_T \frac{1}{T} \frac{\partial T}{\partial r} - D_u \frac{1}{v_{th}} \frac{\partial U_\phi}{\partial r} + V_{pn}$$

Diagram illustrating the decomposition of the particle flux $\frac{\Gamma_n}{n}$ into four terms, each with a colored arrow pointing to its corresponding term in the equation:

- Diffusion** (blue arrow pointing to $-D_n \frac{1}{n} \frac{\partial n}{\partial r}$)
- Thermo-diffusion** (green arrow pointing to $-D_T \frac{1}{T} \frac{\partial T}{\partial r}$)
[Coppi PRL 78, Weiland NF 89]
- Roto-diffusion** (teal arrow pointing to $-D_u \frac{1}{v_{th}} \frac{\partial U_\phi}{\partial r}$)
[Camenen PoP 09, Casson PoP 10]
- Pure convection** (red arrow pointing to $+V_{pn}$)
[Weiland NF 89, Yanko JETP 94, Garbet PRL 03, PoP05]

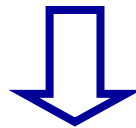
- Interesting property, off-diagonal terms can reverse direction or change parameter dependences depending on the type of turbulence (ITG / TEM)

[review Angioni PPCF 09, all terms from GK : Fable PPCF 10, entropy: Garbet PoP 05]

Electron transport: turbulence produces diffusion & convection



- **Curvature & grad B drift :** $\mathbf{v}_C + \mathbf{v}_{\nabla B} = \frac{v_{\parallel}^2}{\Omega_c} \mathbf{B} \times \mathcal{K}_B + \frac{v_{\perp}^2}{2\Omega_c} \mathbf{B} \times \frac{\nabla B}{B}$
- **Depends on the energy of the particles**
- **Confining magnetic field has gradient and curvature**



- **Exists an off-diagonal term related to the electron temperature gradient (thermo-diffusion)**
- **Exists a pure convective term connected to the magnetic field geometry (“curvature” pinch)**

$$\frac{\Gamma}{n} = -D \frac{\nabla n}{n} - D_T \frac{\nabla T}{T} + V_p$$

- **This is an appropriate physical decomposition, but not a linear relationship**
- **It can be derived consistently from the gyrokinetic equation**

Simple derivation of QL electron flux from the gyrokinetic equation



- **Linearized gyrokinetic equation for electrons**
(ballooning representation, simple Krook collision operator)

$$(\omega - k_{||}v_{||} - \omega_{de} + i\nu_{ei})g = F_M \left\{ \omega_{De} \left[\frac{R}{L_n} + \left(\frac{E}{T_e} - \frac{3}{2} \right) \frac{R}{L_{Te}} \right] - \omega \right\} J_0(k_{\perp}\rho_s)\hat{\phi}$$

- **Compute formally the QL particle flux for trapped electrons ($k_{||} = 0$)**

$$\Gamma_k = \frac{k_y c_s^2}{\Omega_{ci}} \left\langle \int d^3v F_M \frac{(\hat{\gamma}_k + \hat{\nu}_k)[R/L_n + (E/T_e - 3/2)R/L_{Te}] - (\hat{\gamma}_k \hat{\omega}_d - \hat{\omega}_{rk} \hat{\nu}_k)}{(\hat{\omega}_{rk} + \hat{\omega}_d)^2 + (\hat{\gamma}_k + \hat{\nu}_k)^2} J_0(k_{\perp}\rho_s)^2 |\hat{\phi}_k|^2 \right\rangle$$

- **All frequencies normalized to** $\omega_D = k_y \rho_s c_s / R$ **and** $\hat{\omega}_d = \frac{E}{T_e} \left(1 + \frac{v_{||}^2}{v^2} \right) G(\theta)$

Simple derivation for QL electron flux from the gyrokinetic equation



- Linearized gyrokinetic equation for electrons
(ballooning representation, simple Krook collision operator)

$$(\omega - k_{\parallel} v_{\parallel} - \omega_{de} + i\nu_{ei}) g = F_M \left\{ \omega_{De} \left[\frac{R}{L_n} + \left(\frac{E}{T_e} - \frac{3}{2} \right) \frac{R}{L_{Te}} \right] - \omega \right\} J_0(k_{\perp} \rho_s) \hat{\phi}$$

- Compute formally the QL particle flux for trapped electrons

$$\Gamma_k = \frac{k_y c_s^2}{\Omega_{ci}} \left\langle \int d^3 v F_M \frac{(\hat{\gamma}_k + \hat{\nu}_k) \left[\frac{R}{L_n} + \left(\frac{E}{T_e} - \frac{3}{2} \right) \frac{R}{L_{Te}} \right] - (\hat{\gamma}_k \hat{\omega}_d - \hat{\omega}_{rk} \hat{\nu}_k)}{(\hat{\omega}_{rk} + \hat{\omega}_d)^2 + (\hat{\gamma}_k + \hat{\nu}_k)^2} J_0(k_{\perp} \rho_s)^2 |\hat{\phi}_k|^2 \right\rangle$$

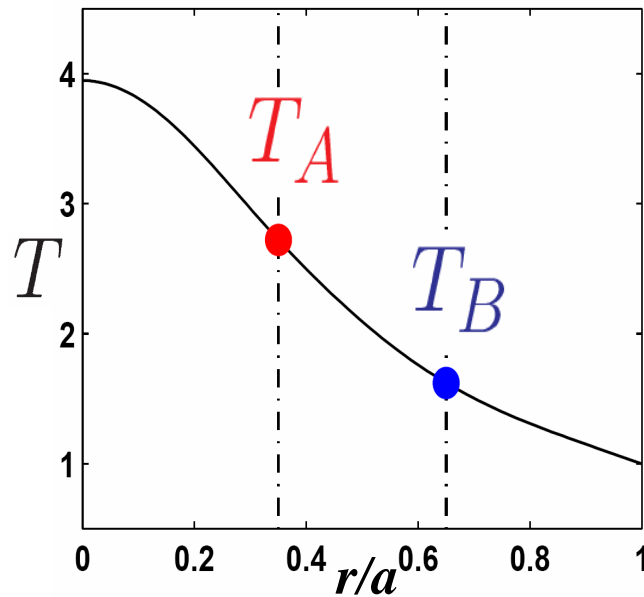
ExB advection
(diffusion, always outward)
Thermo-diffusion
(direction mode dependent)
ExB compression
(pinch)
Collisional term
(mode dependent)

- All frequencies normalized to $\omega_D = k_y \rho_s c_s / R$ and $\hat{\omega}_d = \frac{E}{T_e} \left(1 + \frac{v_{\parallel}^2}{v^2} \right) G(\theta)$

Off-diagonal terms can reverse direction depending on instability, thermodiffusion



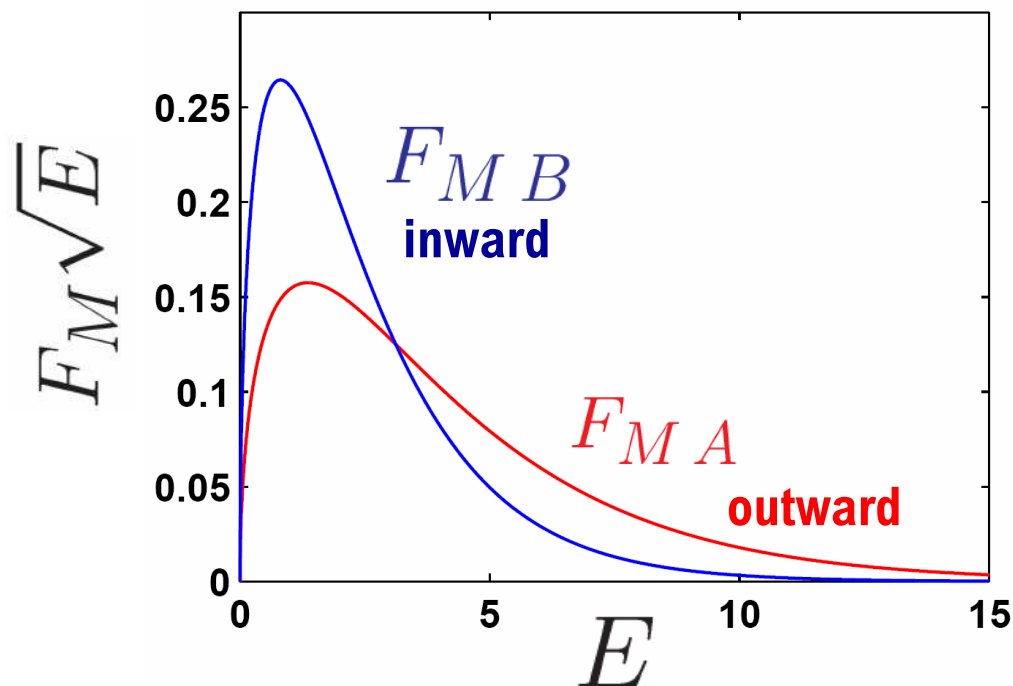
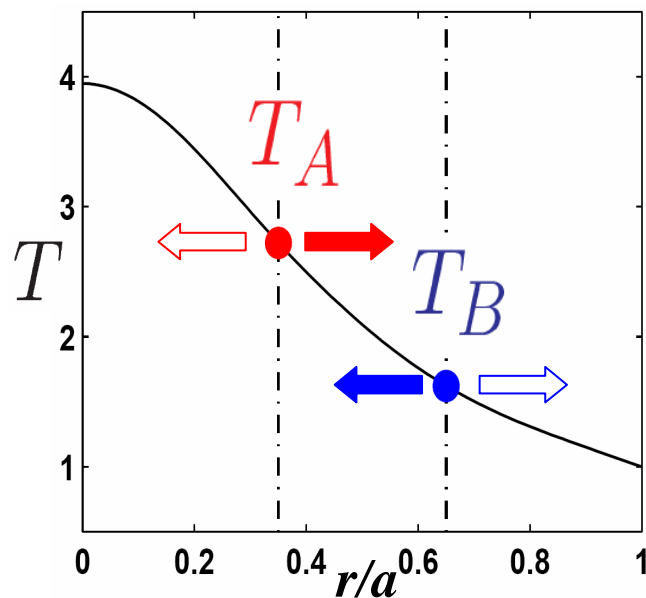
➤ Temperature profile, temperature gradient



Off-diagonal terms can reverse direction depending on instability, thermodiffusion



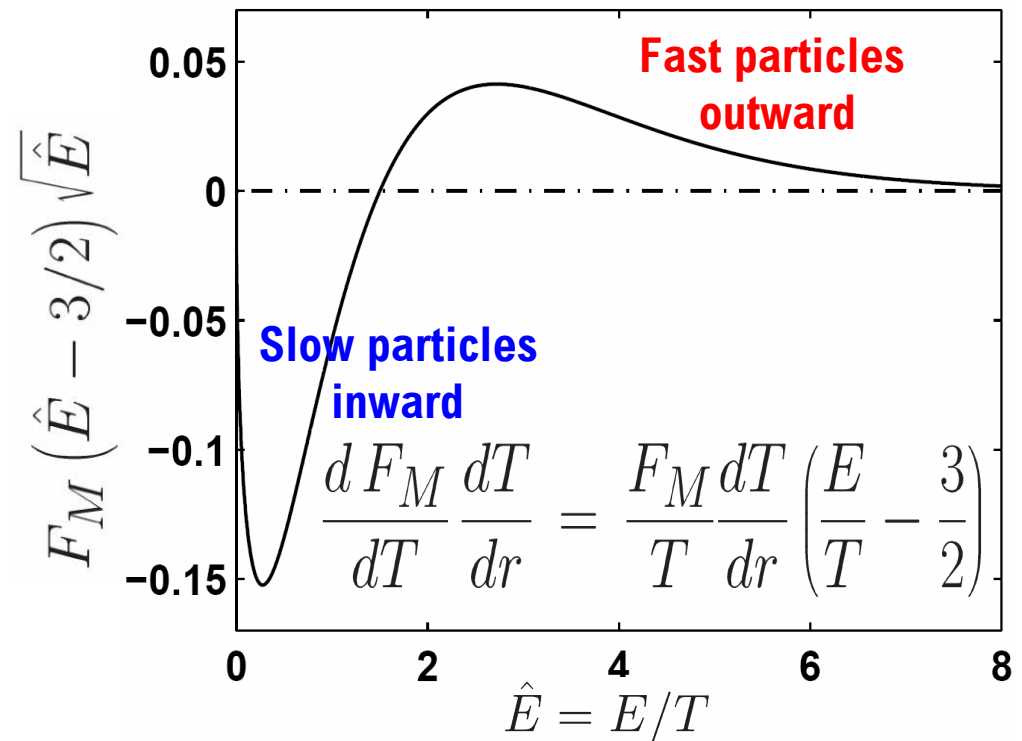
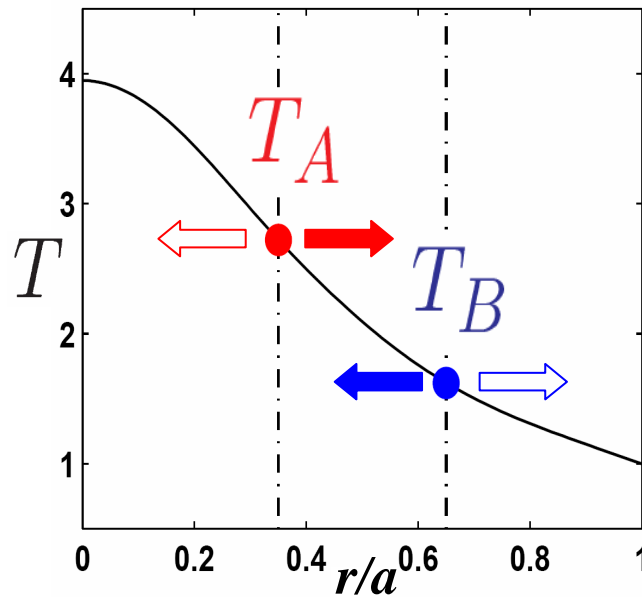
➤ Temperature profile, temperature gradient



Off-diagonal terms can reverse direction depending on instability, thermodiffusion



➤ Temperature profile, temperature gradient



➤ No perturbation, no net flux

➤ Energy dependent perturbation: net flux is produced

➤ Inward for electrons if resonance at low energy (ITG)

➤ Outward for electrons if resonance at sufficiently large energy (TEM)

Contributions inward or outward, for electrons and impurities, produce a complex pattern



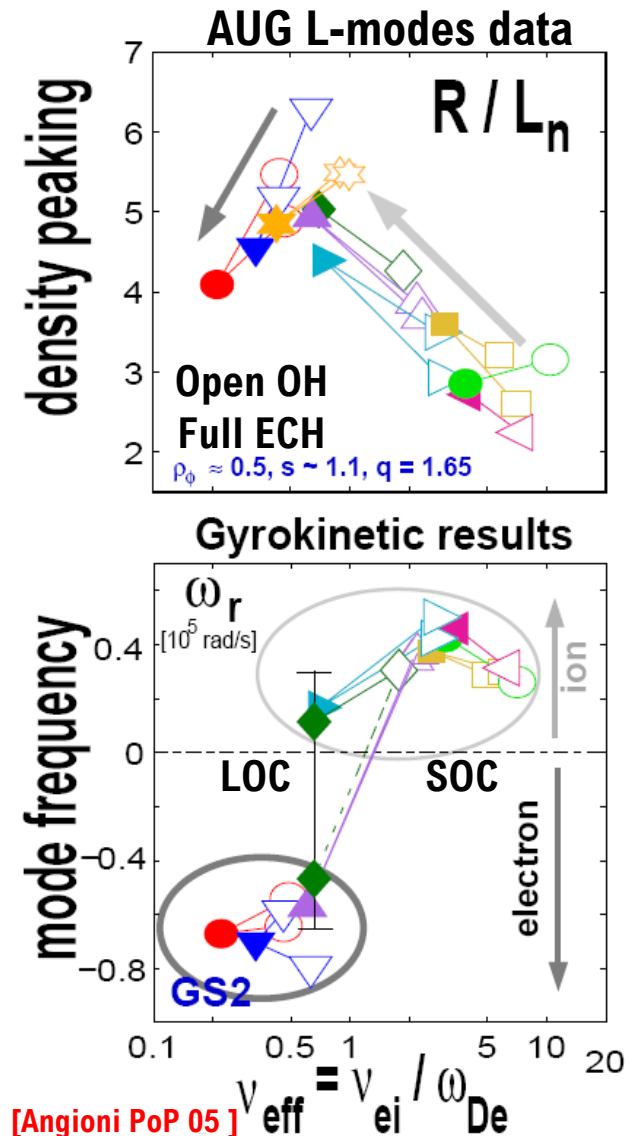
		Thermodiffusion		Pure Convection		Collisions (electron) Roto-diffusion (imp)	
		ITG	TEM	ITG	TEM	ITG	TEM
Curvature & ∇B resonance only	electrons	in	out	in		out	in
	impurities	out	in			out	in
slab resonance limit	electrons	in		out	in	out	in
	impurities			in	out	out	in

- Framework for theory validation : do experiments exhibit the same pattern ?
- Centrifugal effects complicate the picture even more for heavy impurities
[Camenen PoP 09, Casson PoP 10, Veth in prep.]

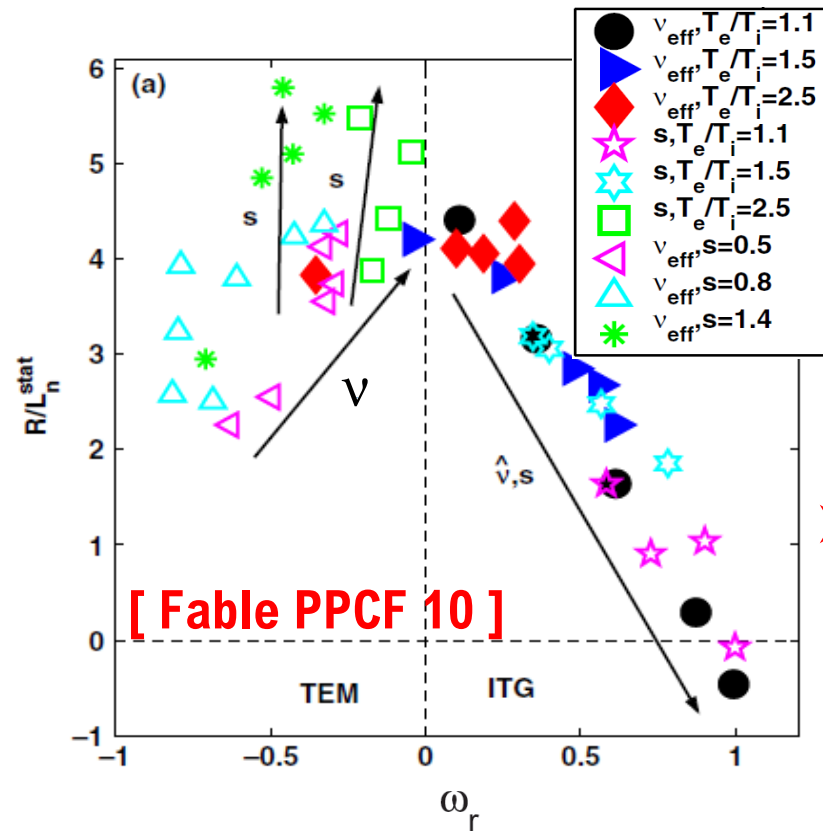
Central ECH can flatten or peak the density profile depending on the turbulence type



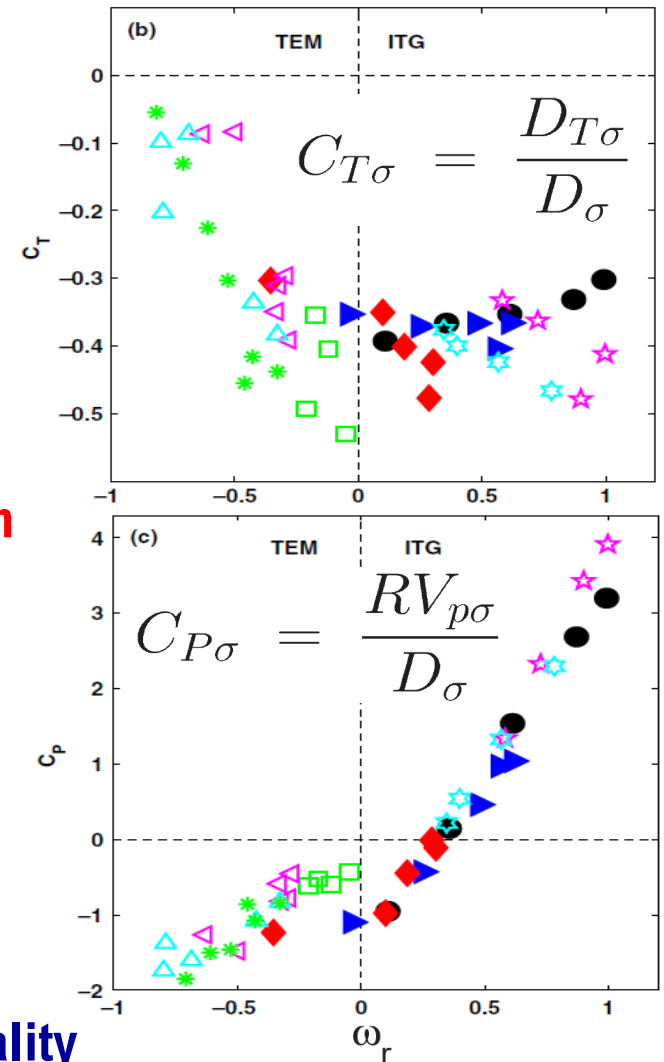
- Different response of density peaking to central ECH can be explained by reversal of thermo-diffusion from inward (ITG) to outward (strong TEM)
[Angioni NF 04, PoP 05]
- ITG, peaking increases in response to central ECH
- destabilization of strong TEM, peaking decreases with central ECH
- Concurrent analysis of electron heat transport finds consistent conclusions [Ryter PRL 05]
- ... and relationship with LOC – SOC regimes [Angioni PoP 05]
- Agrees with results obtained in TORE SUPRA [Hoang PRL 04] and FTU [M. Romanelli PPCF 07]



Theoretical dependences of density peaking on various parameters captured by the mode frequency

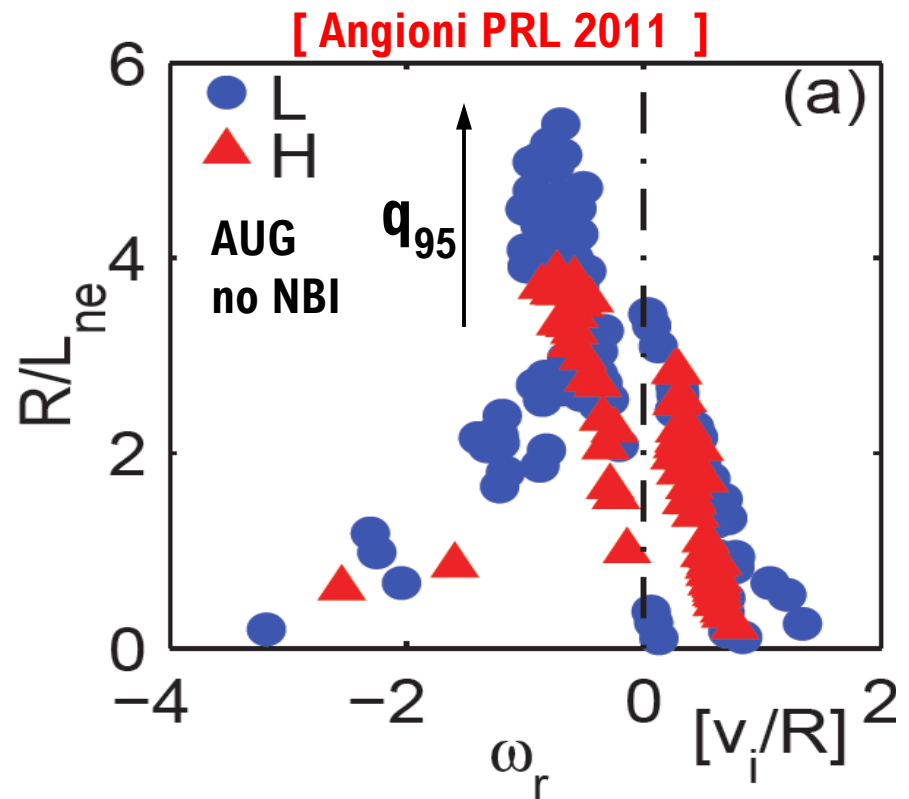
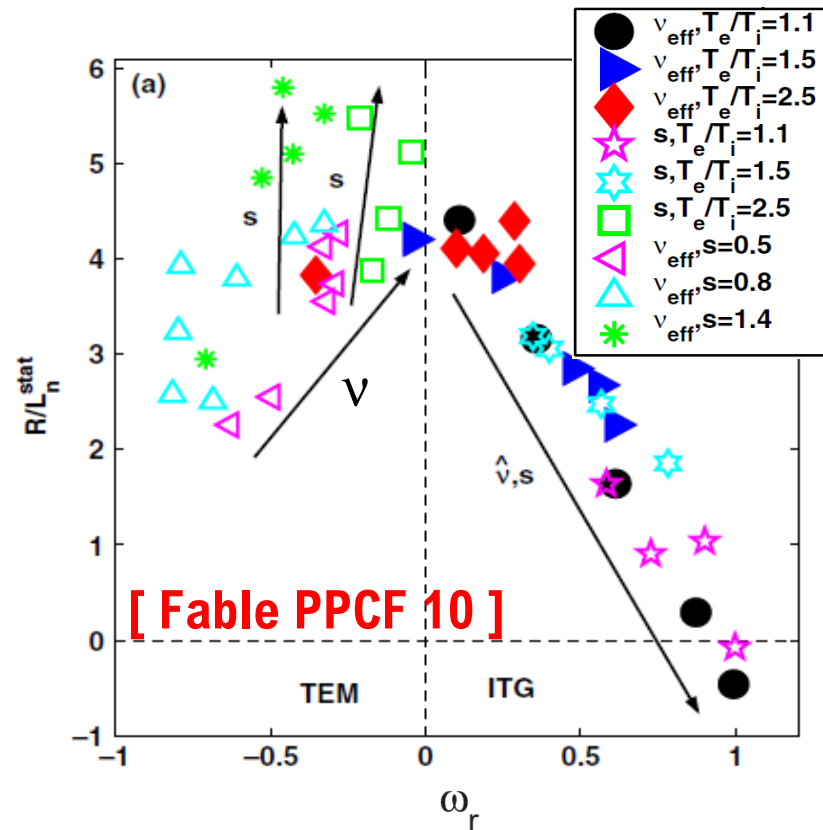


➤ Max peaking in TEM, close to TEM-ITG transition



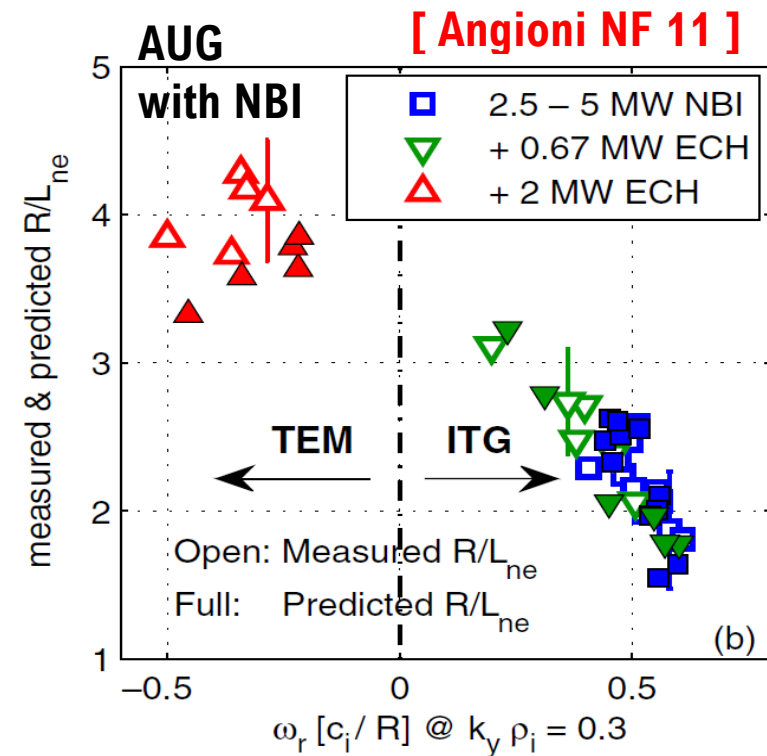
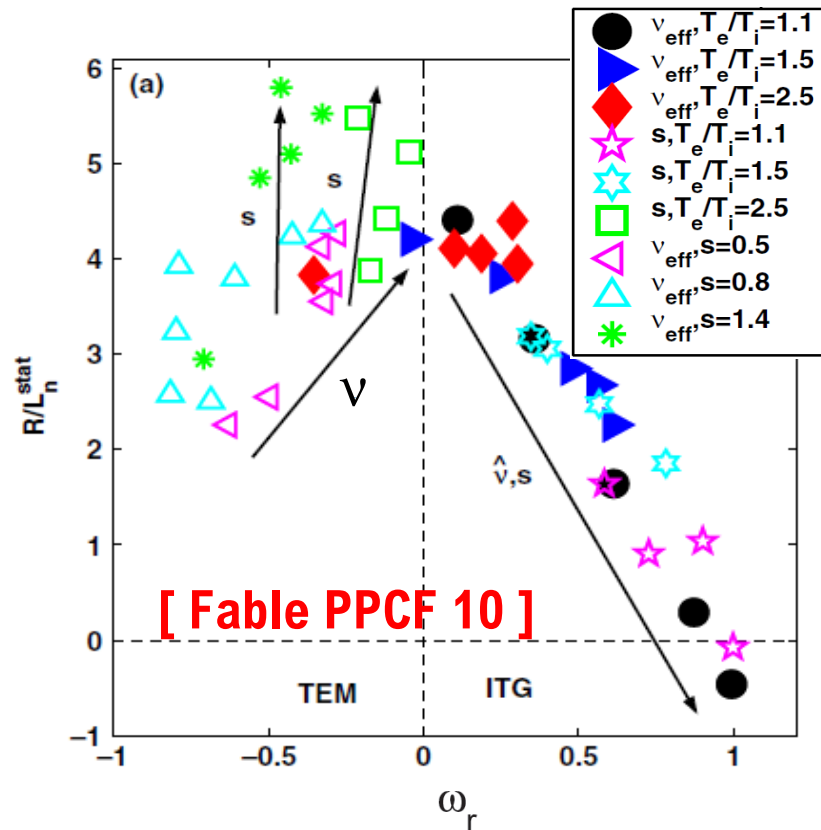
- Due to collisions, pure convection coefficient C_p increases (outward) with increasing mode frequency
- Density peaking decreases with increasing collisionality in ITG, observed in many devices (H-mode) [Angioni PPCF 09]

Experimental data (in both L-mode and H-mode) follow predicted dependence on mode frequency



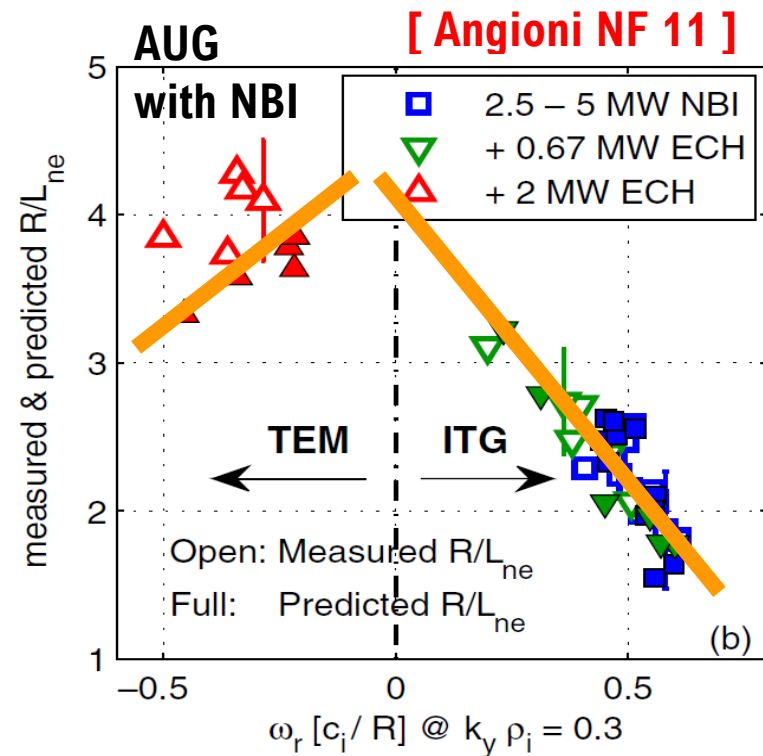
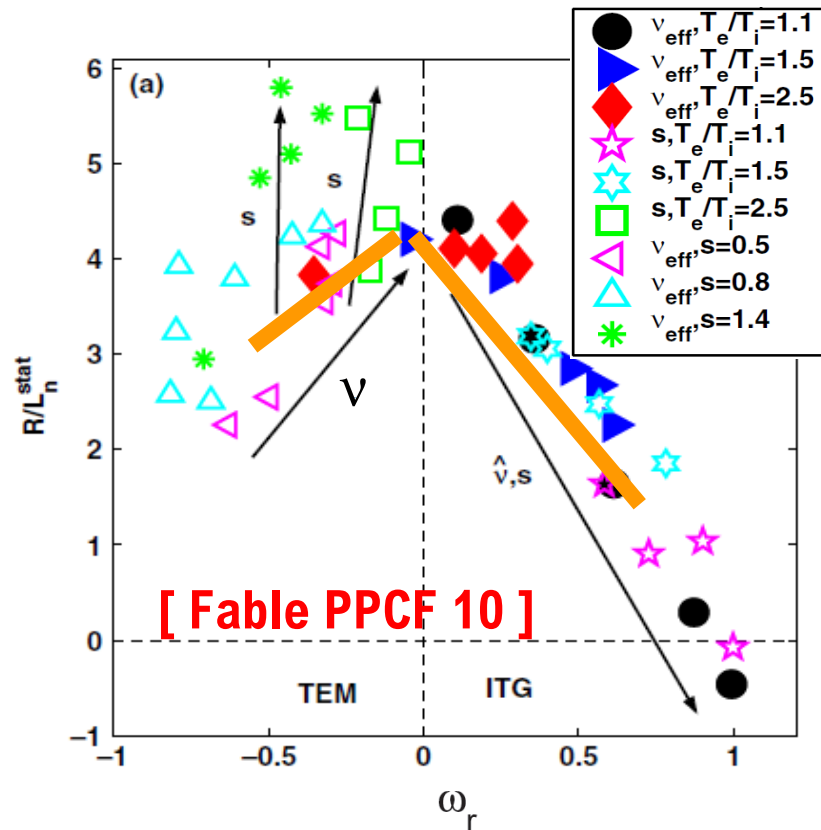
- Predicted curve describing dependence of peaking on mode frequency followed by a large database of observations in L- and H-mode
- In TEM turbulence, peaking predicted to increase with increasing magnetic shear, consistent observations in many devices (L-mode) **[Angioni PPCF 09 for a review]**

Dedicated modelling of specific data follow the same curve, and demonstrate quantitative match



- Explains (& predicts) why central ECH increases density peaking with ITG modes
- Increase of L_{Ti}/L_{Te} , T_e/T_i and drop of collision frequency reduce mode frequency & increase peaking

Dedicated modelling of specific data follow the same curve, and demonstrate quantitative match



- Explains (& predicts) why central ECH increases density peaking with ITG modes
- Increase of LT_i/LT_e , T_e/T_i and drop of collision frequency reduce mode frequency & increase peaking

Impurity transport: charge & mass provide additional handle to identify different processes

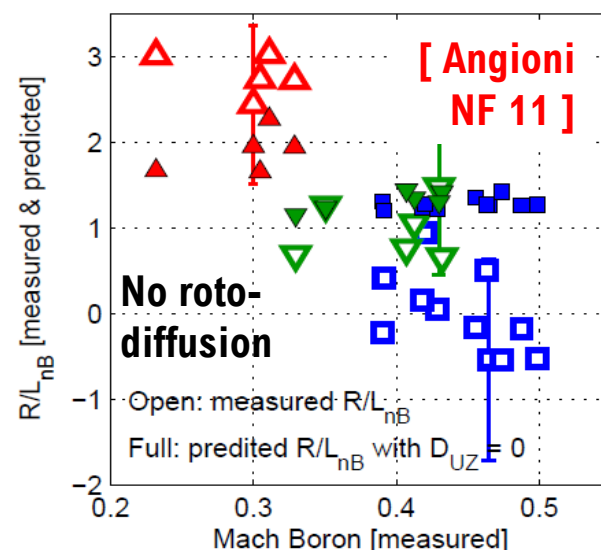
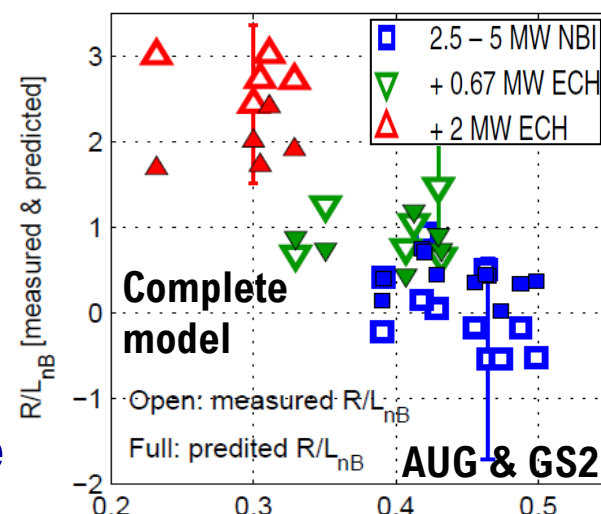


- Dependences on Z and A arise from the resonances, provided by the perpendicular and parallel gyro-centre motions

[Angioni PRL 06, Dubuit PoP 07, Bourdelle PoP 07, ...]

- Rotational / centrifugal effects & poloidal asymmetries strongly impact the dependences of the transport coefficients for heavy impurities

[Camenen PoP 09, Casson PoP 10, Fulop PoP 11, Moradi PPCF 11, Veth in prep.]



- Roto-diffusion directly links impurity transport to toroidal momentum transport

- Roto-diffusion outward in ITG, contributes to flatten the impurity density profile of rotating plasmas

[Angioni NF 11]

- First indication, further studies required

Outline

- A pragmatic approach, general expressions of particle and toroidal momentum fluxes, similarities and differences
- Main implications on the phenomenology, key observations, back implications on theory
- **One step further, deeper in physical understanding**
- **Nature of different off-diagonal mechanisms, experimental evidences, main parametric dependences, open questions**
 - Particle (& impurity) transport
 - **Toroidal momentum transport**
- Impact of different turbulent regimes on non-diffusive particle and momentum transport (similarities & differences), relevance in the core (and at the edge)

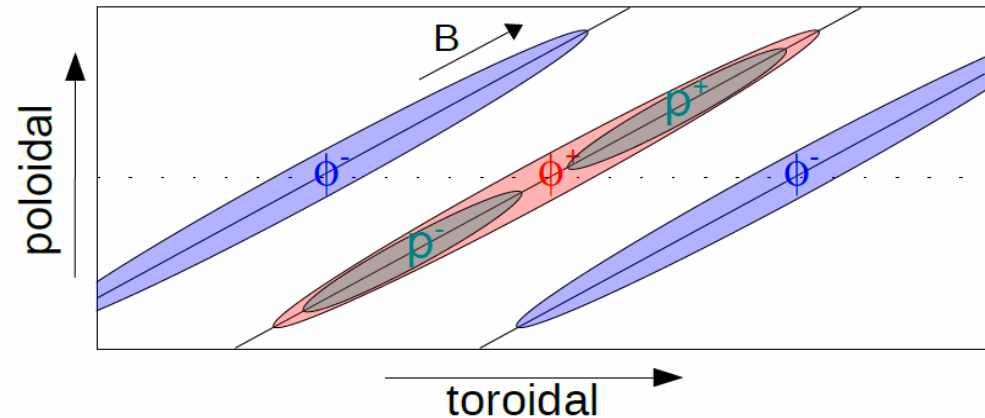
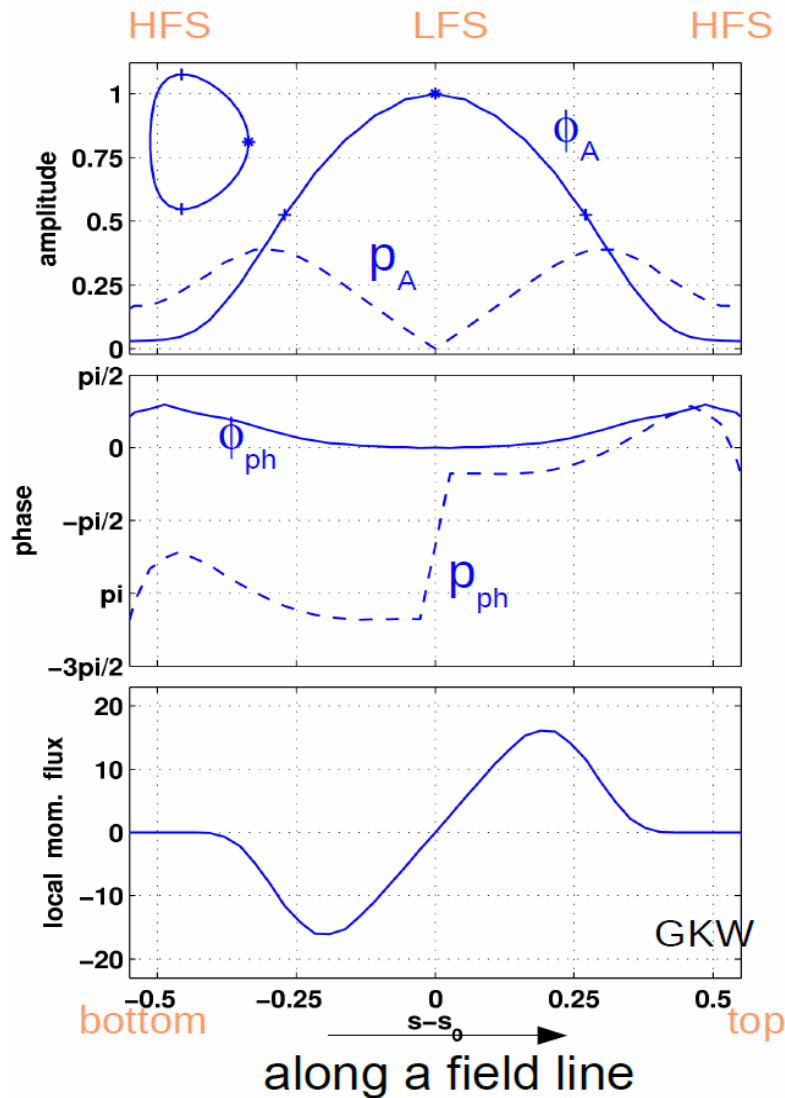
Decomposing the expressions of the fluxes, toroidal momentum transport



- **Toroidal momentum flux : odd velocity moment, component of a vectorial quantity, in contrast to density and energy, it can be positive or negative ... co-current or counter-current, co-field or counter-field**
- **Off-diagonal terms are zero unless a mechanism is present which breaks symmetry properties that the solution of the gyrokinetic equation has in a local limit**

[Peeters PoP 05, NF 11, Diamond PoP 08, Parra PoP 11, Staebler PoP 11]

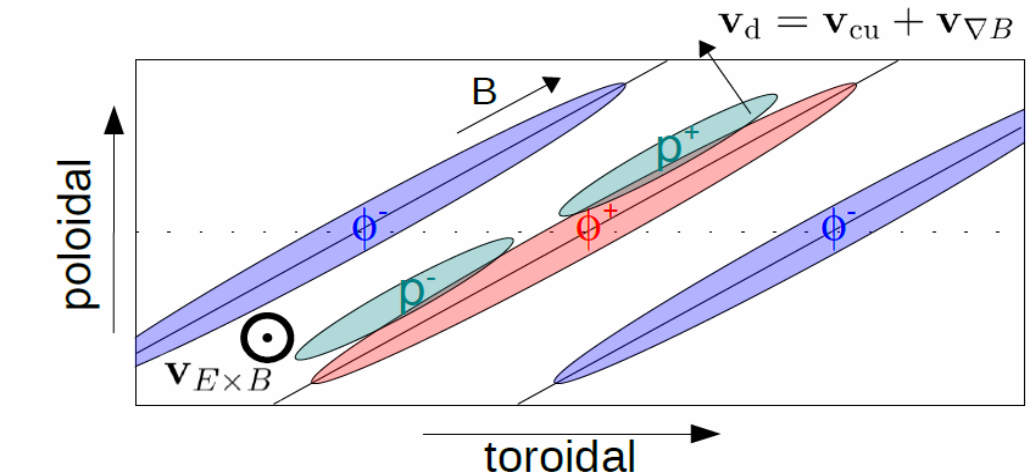
The symmetry properties (linear picture)



- ▶ Parallel acceleration by the perturbed potential gradient
→ parallel velocity perturbation
- ▶ Parallel velocity moment:

$$p = 2\pi B \int m v_{\parallel} f dv_{\parallel} d\mu$$

[Courtesy of Y. Camenen, EFTC 2009]



- ▶ Perp. drift of the $p_{||}$ perturbation and ExB advection \rightarrow local flux of momentum
- ▶ But $f(v_{||}, s) = f(-v_{||}, -s)$ [Peeters PoP2005]

$$\Gamma_{\parallel} = \left\langle \underbrace{2\pi B \int \nabla r \cdot \mathbf{v}_E}_{\text{symmetric}} \underbrace{m v_{\parallel} f \, dv_{\parallel} \, d\mu}_{\text{anti-symmetric}} \right\rangle$$

**Exact compensation over the FS average
→ no net radial flux of momentum
Symmetry breaking mechanism required!**

Symmetry breaking, conditions for non zero off-diagonal terms in the toroidal momentum flux



[Peeters NF 11, Parra PoP 11]

➤ The transformation

$$v_{\parallel} \rightarrow -v_{\parallel} \quad s \rightarrow -s \quad r \rightarrow -r \quad f \rightarrow -f \quad \phi \rightarrow -\phi \quad \delta A_{\parallel} \rightarrow \delta A_{\parallel} \quad \delta B_{\parallel} \rightarrow -\delta B_{\parallel}$$

➤ changes the sign of the toroidal momentum flux, while keeping the gyrokinetic equation invariant, provided the following conditions are satisfied

✓ **Lowest order terms in ρ^* (no parallel velocity nonlinearity, no profile shearing or radial variation of turbulence intensity)**

✓ $\frac{\partial \omega_{\phi}}{\partial r} = 0$; $\omega_{\phi} = 0$; $\gamma_E = 0$;

✓ **Up-down symmetric equilibrium**

➤ If any of these conditions is not satisfied, the gk equation is no longer invariant, and the symmetry properties of the solution are broken

➤ A finite momentum flux can be generated (necessary but not sufficient condition)

Decomposing the expressions of the fluxes, toroidal momentum transport [Peeters NF 11, Staebler PoP 11]



- Toroidal momentum flux : off-diagonal terms are zero unless a mechanism breaking the parallel symmetry is present (obviously particle flux always present)

$$\frac{\Pi_\phi}{nmR} = -\chi_{\phi\parallel} R \frac{\partial \omega_\phi}{\partial r} + \left(V_\phi + \frac{\Gamma_n}{n} \right) R \omega_\phi + \frac{\Pi_{FS}}{nmR} + M_\parallel \gamma_E + \rho_*^\alpha \frac{\Pi_*}{nmR}$$

Parallel velocity shear [Matter PF 88, Peeters PoP 05] (points to $-\chi_{\phi\parallel}$)
 Pinch [Peeters PRL 07, Hahn PoP 07, Waltz PoP 07] (points to V_ϕ)
 Particle flux (points to $\frac{\Gamma_n}{n}$)
 Up-down asymmetry [Camenen PRL 09] (points to Π_{FS})
 ExB shearing [Dominguez PFB 93, Gurcan PoP 07, Waltz PoP 09, Casson PoP 09] (points to M_\parallel)
 Finite ρ^* (points to ρ_*^α)

- Mechanisms of symmetry breaking allow a physical decomposition of the off-diagonal contributions
- No direct off-diagonal terms due to density or temperature gradients, they do not break the symmetry

The (Coriolis) pinch

[Peeters PRL 07, Hahm PoP 07, Waltz PoP 07]



$$\frac{\Pi_\phi}{nmR} = -\chi_{\phi\parallel} R \frac{\partial \omega_\phi}{\partial r} + \left(\boxed{V_\phi} + \frac{\Gamma_n}{n} \right) \boxed{R\omega_\phi} + \frac{\Pi_{FS}}{nmR} + M_\parallel \gamma_E + \rho_*^\alpha \frac{\Pi_*}{nmR}$$

Parallel velocity shear
[Mattor PF 88, Peeters PoP 05]

Particle flux

Pinch
[Peeters PRL 07,
Hahm PoP 07,
Waltz PoP 07]

Up-down asymmetry
[Camenen PRL 09]

ExB shearing
[Dominguez PFB 93, Garbet PoP 02,
Gurcan PoP 07,
Waltz PoP 09, Casson PoP 09]

Finite ρ^*

➤ Symmetry breaking through parallel/toroidal flow

Coriolis pinch: symmetry breaking necessary but not sufficient



- In the co-moving frame, a background rotation produces inertial drifts

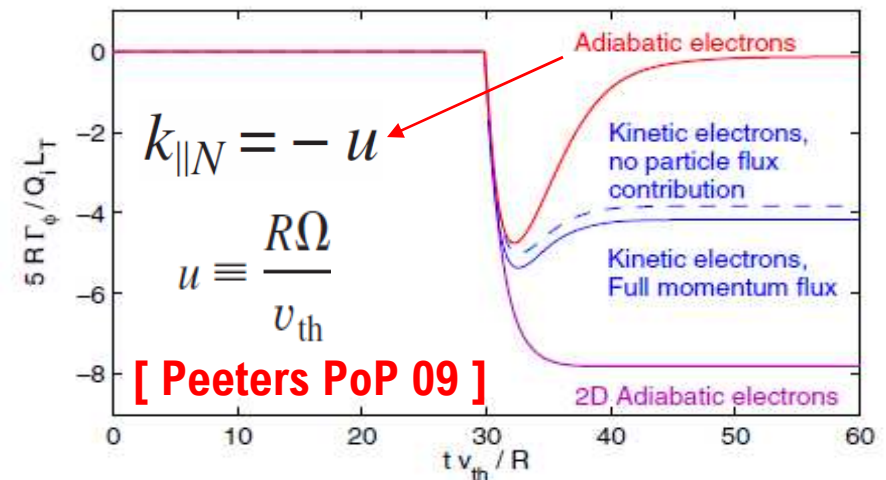
$$\mathbf{v} = \frac{\mathbf{F} \times \mathbf{B}}{ZeBB_{\parallel}^*} \quad \mathbf{F}_{co} = 2mv_{\parallel} \mathbf{b} \times \boldsymbol{\Omega} \quad \mathbf{v}_{co} = 2 \frac{mv_{\parallel}}{ZeB_{\parallel}^*} \boldsymbol{\Omega}_{\perp}$$

Drift equation Coriolis force **Coriolis drift**

$$\frac{\partial f}{\partial t} + v_{\parallel} \mathbf{b} \cdot \nabla f + \mathbf{v}_d \cdot \nabla f + \mathbf{v}_{\text{Coriolis}} \cdot \nabla f =$$

$$-\mathbf{v}_E \cdot \nabla f - \frac{eF_M}{T} \left[v_{\parallel} \mathbf{b} + \mathbf{v}_d + \mathbf{v}_{\text{Coriolis}} \right] \cdot \nabla \phi$$

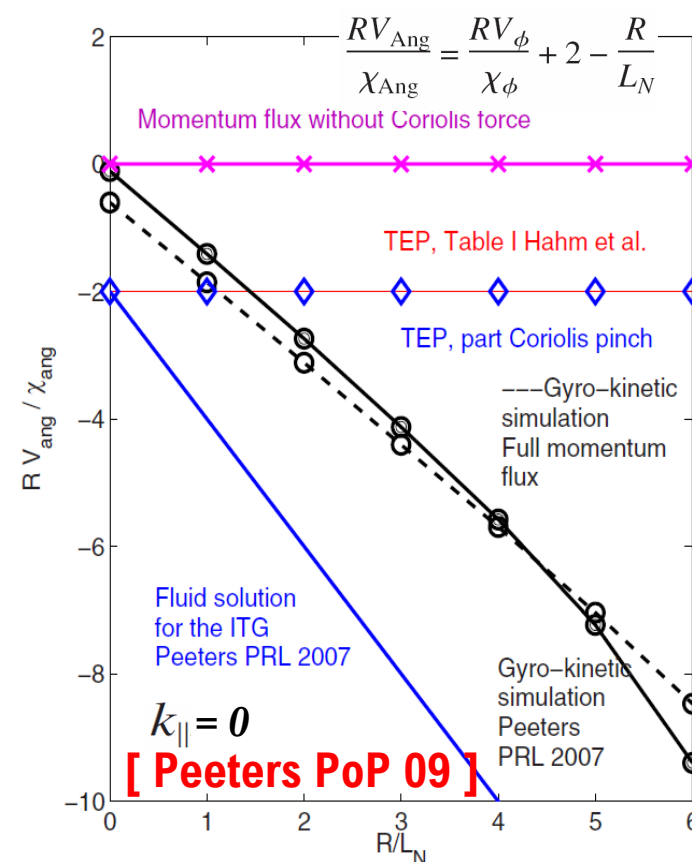
- Parallel streaming (k_{\parallel}) and Coriolis drift appear always in pairs
- Mode adjusts and compensates asymmetry produced by Coriolis drift
- With adiabatic electrons, full compensation, no pinch



Coriolis pinch: symmetry breaking necessary but not sufficient, requires self-consistent mode structure



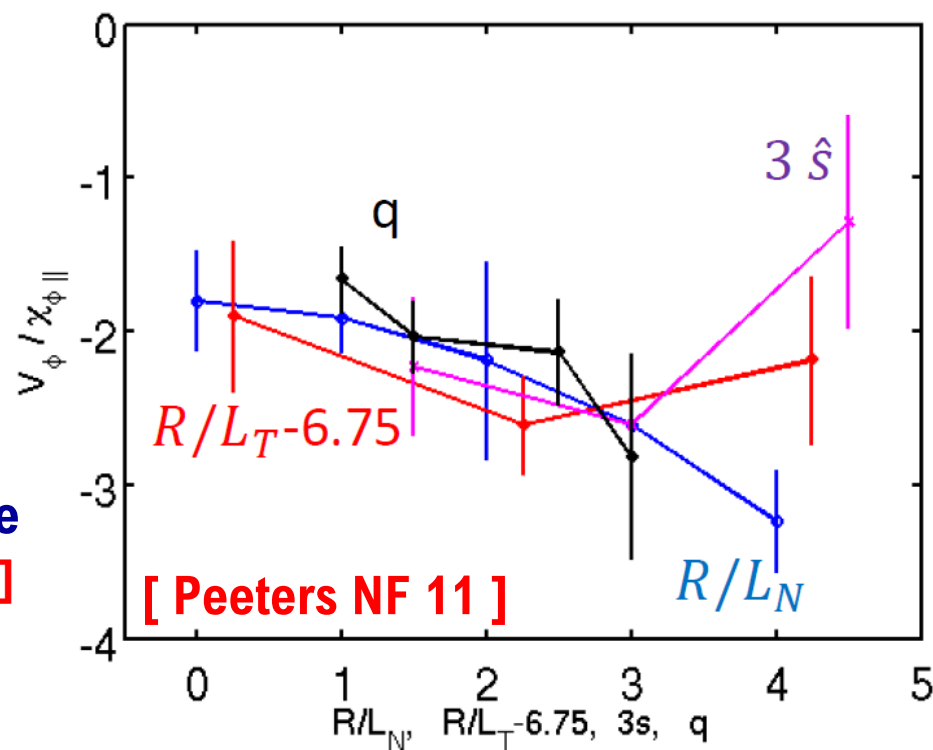
- With trapped electrons the compensation is only partial, and a pinch remains
- Quantitative comparisons with the experiment to be performed **ONLY** with calculations which include the self-consistent mode structure (self-consistent $k_{||}$)
- Models which assume $k_{||} = 0$ (e.g. simple fluid formulae which neglect self-consistent mode structure) largely overestimate the pinch (not suited for comparisons with experiments)
- These simple models remain useful for physics understanding
- Have been used for first comparisons with experiment [Solomon PRL 08, Kaye NF 2010]
- At this stage, self-consistent (gk/gf) calculations can and should be performed



Coriolis pinch: main parameter dependences in the theoretical predictions



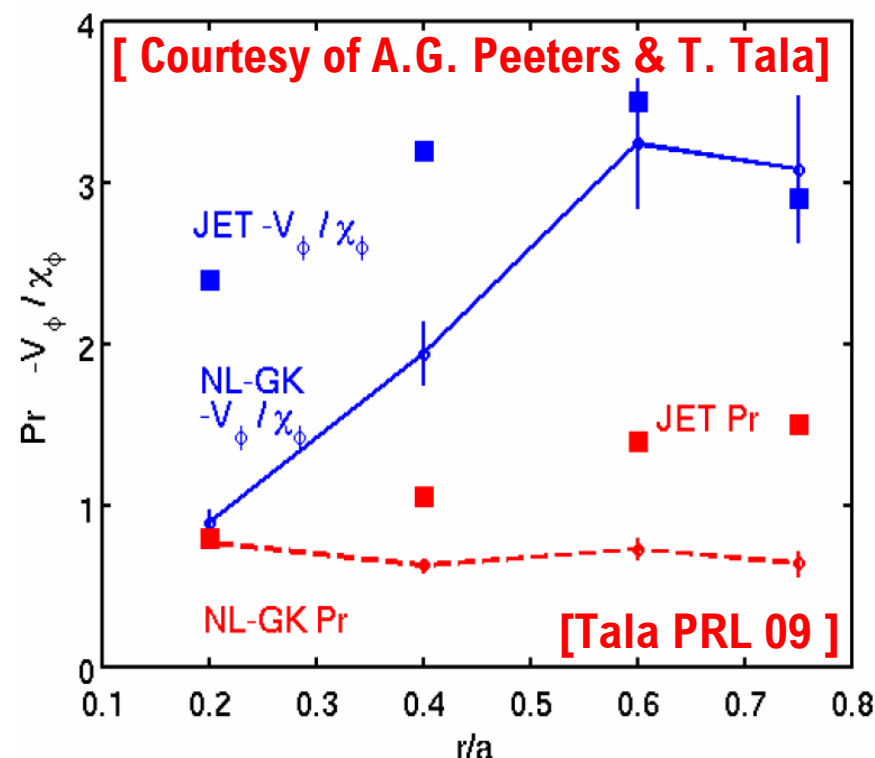
- The Coriolis term is a pinch (it is directed inward, increases the rotation regardless its direction)
- Compensation effects produce almost linear dependence on $\sqrt{\epsilon}$
- Coriolis drift is vertical, requires LFS localization of mode. This implies geometric dependences (s & q)
- Main dependence is on R/L_n , weak dependence on R/L_T
- Dependence on ν & β weak at low ν & β , become stronger at high ν & β (close to KBM) $\langle k_{||} \rangle = \langle k_{||} \rangle(\beta)$ [Hein PoP 11]
- Dependences imply pinch is small close to the center, becomes larger in the confinement region



Coriolis pinch: main parameter dependences in the theoretical predictions



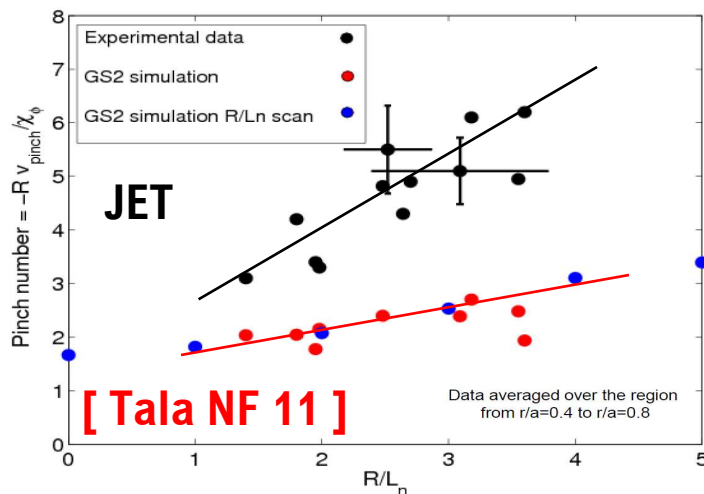
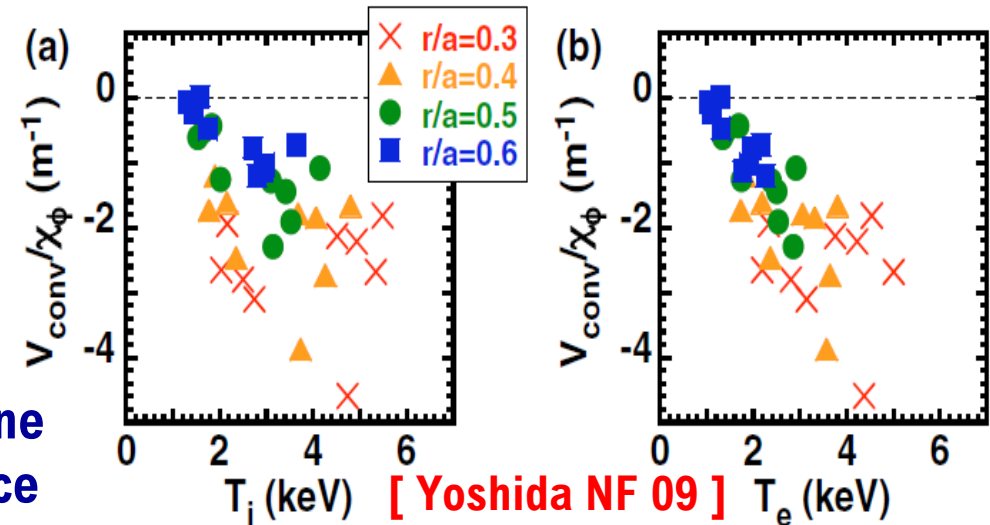
- The Coriolis term is a pinch (it is directed inward, increases the rotation regardless its direction)
- Compensation effects produce almost linear dependence on $\sqrt{\varepsilon}$
- Coriolis drift is vertical, requires LFS localization of mode. This implies geometric dependences (s & q)
- Main dependence is on R/Ln , weak dependence on R/LT
- Dependence on ν & β weak at low ν & β , become stronger at high ν & β (close to KBM) $\langle k_{||} \rangle = \langle k_{||} \rangle(\beta)$ [Hein PoP 11]
- Dependences imply pinch is small close to the center, becomes larger in the confinement region



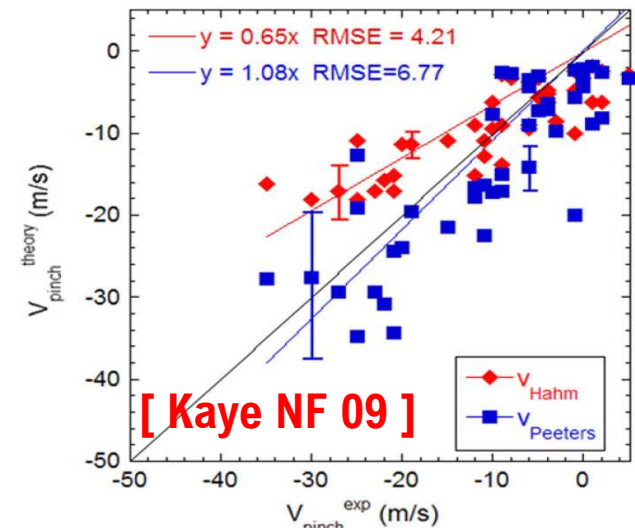
In the experiments, main parameter dependences of the pinch and comparison with theory



- Modulation experiments to evaluate the pinch and study parametric dependences in the experiments
- Experiment analyzed assuming that residual stress is negligible
- In JT-60U dependences on T_i, T_e and n_e & T gradients, in JET main dependence on R/L_n , stronger than in the theoretical prediction



Weak dependence of pinch number vs collisionality
[DIII-D & NSTX
Solomon PoP 10,
JET Tala NF 11]



- Predicted pinch (& Pr) number usually too small

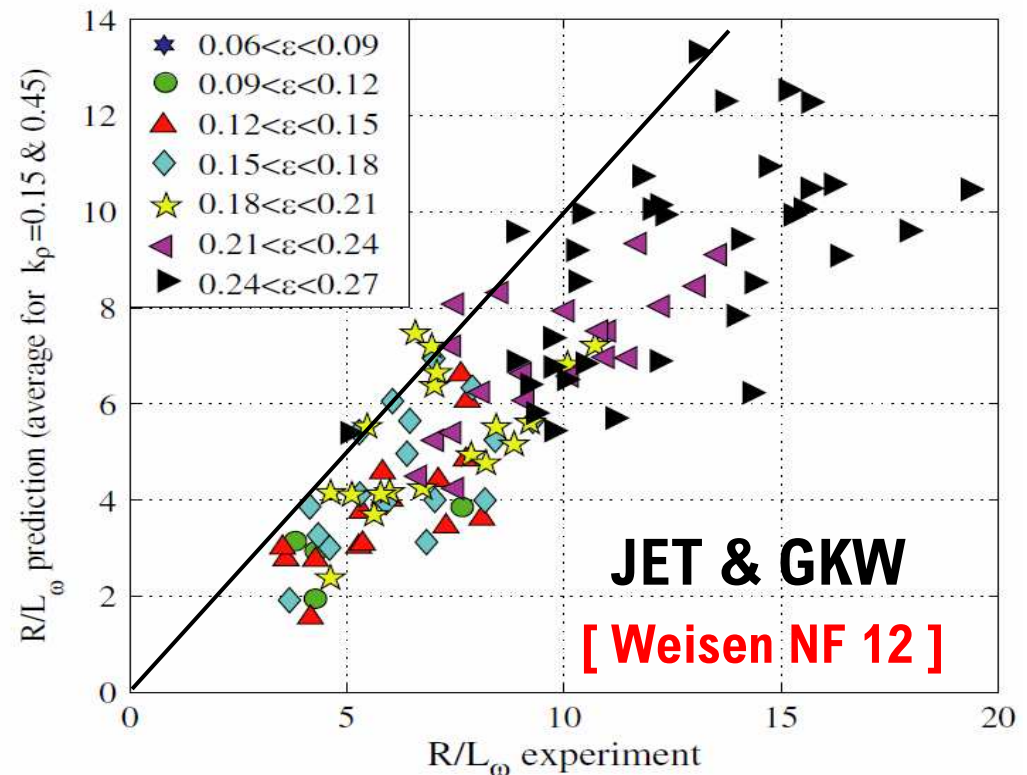
Alternative approach on database of JET NBI heated plasmas, allows identification of Coriolis pinch



- Large database of JET observations in the presence of NBI heating

- Multivariate regressions deliver average Pr and dependences of pinch number

- Dependences of pinch number consistent with theoretical predictions for Coriolis pinch



- On average pinch number predicted 30% too small, agreement increases for subsets with large Mach numbers
- Agreement with theory allows experimental identification of Coriolis pinch mechanism

The particle flux

[Gurcan PoP 07]



$$\frac{\Pi_\phi}{nmR} = -\chi_{\phi\parallel} R \frac{\partial \omega_\phi}{\partial r} + \left(V_\phi + \frac{\Gamma_n}{n} R \omega_\phi \right) + \frac{\Pi_{FS}}{nmR} + M_\parallel \gamma_E + \rho_*^\alpha \frac{\Pi_*}{nmR}$$

Parallel velocity shear
 [Matter PF 88, Peeters PoP 05]

Pinch
 [Peeters PRL 07, Hahn PoP 07, Waltz PoP 07]

Particle flux

Up-down asymmetry
 [Camenen PRL 09]

ExB shearing
 [Dominguez PFB 93, Garbet PoP 02, Gurcan PoP 07, Waltz PoP 09, Casson PoP 09]

Finite ρ^*

➤ No symmetry breaking required, normal convection

Particle Flux in toroidal momentum flux

- **Directly connects momentum transport to the particle flux**
- **In stationary conditions, particle flux is usually small (negligible) in the core, even in the presence of beams, but can be large at the edge (depends on penetration of ionization source, or depends on use of fuelling methods with higher penetration)**
- **It is directed outward (in stationary conditions it is the volume integral of the particle source), opposite effect to the Coriolis pinch**
- **Experiments in which core particle sources are applied (e.g. pellets) could be of interest also for momentum transport**
 - **Because they generate a particle flux in the core**
 - **Because they lead to the formation of stronger gradients of the density profiles which are not produced in the presence of zero particle source. This can be a tool for the investigation of the impact of density profiles on momentum transport**

The up-down asymmetry

[Camenen PRL 09, PoP 09, PRL 10]



$$\frac{\Pi_\phi}{nmR} = -\chi_{\phi\parallel} R \frac{\partial \omega_\phi}{\partial r} + \left(V_\phi + \frac{\Gamma_n}{n} \right) R \omega_\phi + \boxed{\frac{\Pi_{FS}}{nmR}} + M_\parallel \gamma_E + \rho_*^\alpha \frac{\Pi_*}{nmR}$$

Parallel velocity shear
 [Matter PF 88, Peeters PoP 05]

Pinch
 [Peeters PRL 07, Hahn PoP 07, Waltz PoP 07]

Particle flux

Up-down asymmetry
 [Camenen PRL 09]

ExB shearing
 [Dominguez PFB 93, Garbet PoP 02, Gurcan PoP 07, Waltz PoP 09, Casson PoP 09]

Finite ρ^*

➤ Symmetry breaking by asymmetry of the geometrical configuration

Up-down asymmetry of the magnetic configuration,



$$\Gamma_{\parallel} = \left\langle 2\pi B \int \nabla r \cdot \mathbf{v}_E m v_{\parallel} f dv_{\parallel} d\mu \right\rangle$$

- ▶ Parallel velocity moment:

$$p = 2\pi B \int m v_{\parallel} f dv_{\parallel} d\mu$$

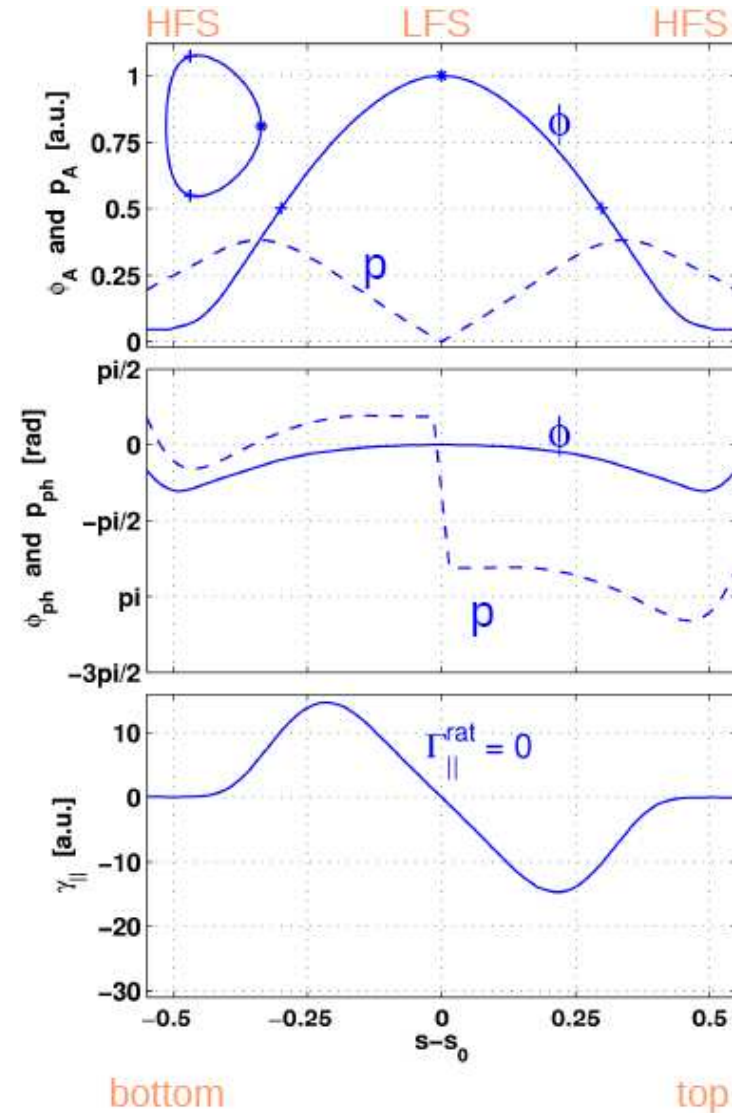
- ▶ “s” is the parallel coordinate

- ▶ Flux surface average:

$$\langle A \rangle = \oint A ds$$

In the absence of
parallel symmetry breaking:

$$\Gamma_{\parallel} = 0$$



[Camenen PRL 09, PoP 09]

Up-down asymmetry of the magnetic configuration

$$\Gamma_{\parallel} = \left\langle 2\pi B \int \nabla r \cdot \mathbf{v}_E m v_{\parallel} f dv_{\parallel} d\mu \right\rangle$$

- ▶ Parallel velocity moment:

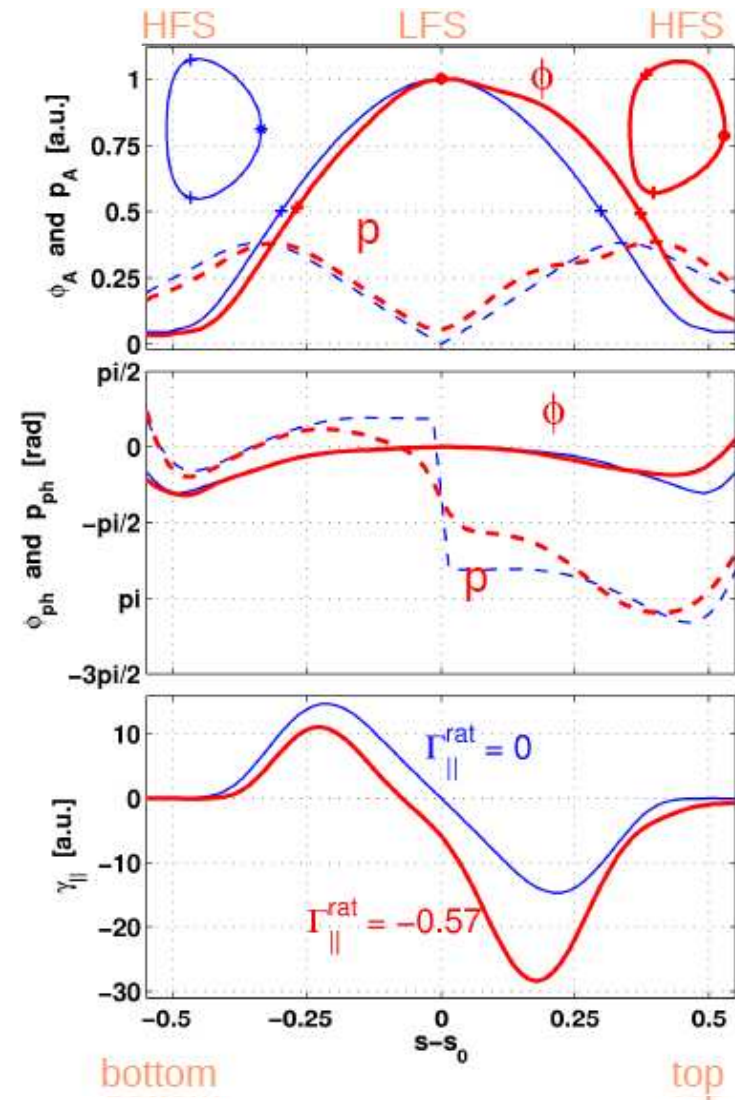
$$p = 2\pi B \int m v_{\parallel} f dv_{\parallel} d\mu$$

- ▶ “s” is the parallel coordinate

- ▶ Flux surface average:

$$\langle A \rangle = \oint A ds$$

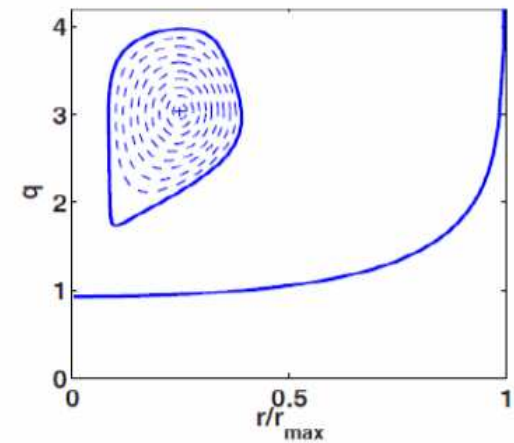
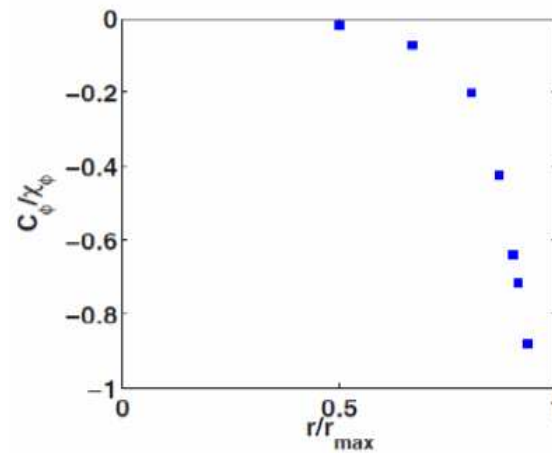
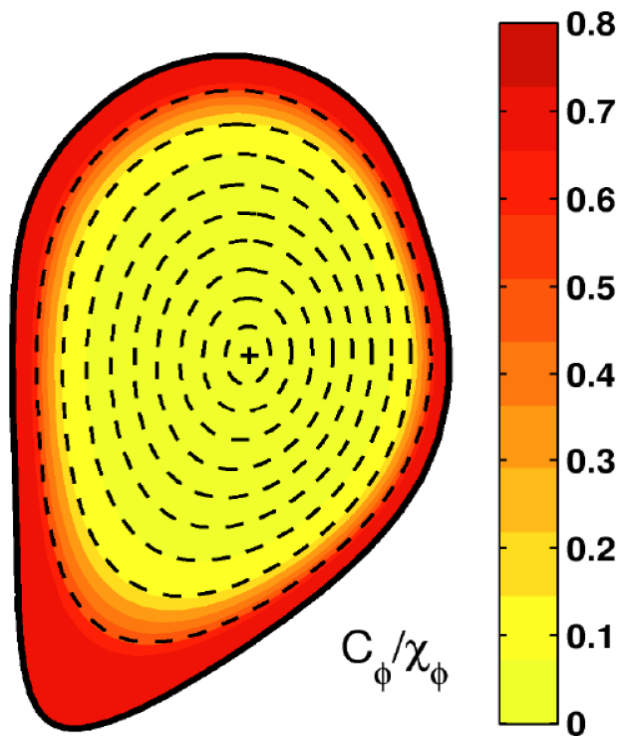
**Compensation over
the FS average is incomplete:
NET MOMENTUM FLUX GENERATED**



[Camenen PRL 09, PoP 09]

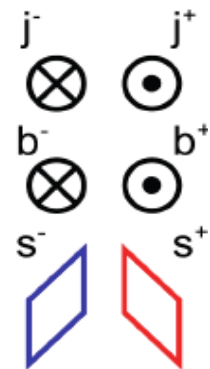
Up-down asymmetry of the magnetic configuration

- Effect is sizeable only at the edge, but can contribute to provide edge seed rotation (residual stress at the boundary), transported in the core by the pinch
- Small for usual up-down asymmetry of diverted tokamaks



➤ Changes sign if

- ▶ I_p direction is reversed
- ▶ B_T direction is reversed
- ▶ shape is reversed



[Camenen PRL 09, PoP 09]

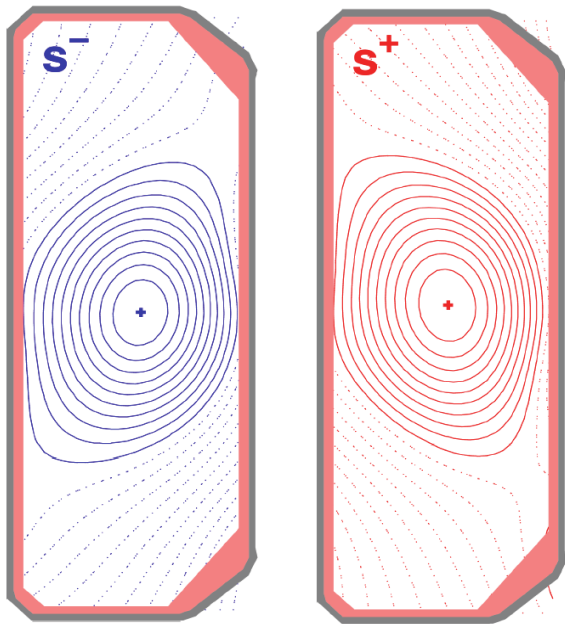
Validated by experiments in TCV

[Camenen PRL 10, PPCF 10]



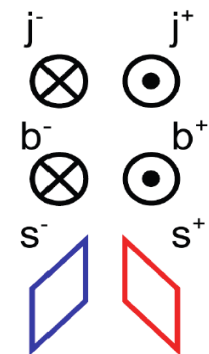
► **Theory** : up-down asymmetry → residual stress [Camenen PRL09, PoP09]

$$-R_0 \frac{\partial \omega_\varphi}{\partial r} = -\frac{R_0 V_{co}}{\chi_\varphi} \omega_\varphi - \frac{C_{other}}{\chi_\varphi} \boxed{-\frac{C_{FS}}{\chi_\varphi}}$$



► **Prediction:** C_{FS} changes sign if

- I_p direction is reversed
- B_T direction is reversed
- shape is reversed



► **Scenario:** explore the 8 configurations, look at the rotation gradient variation

► **Experiments** in the TCV tokamak: extended shaping capabilities and intrinsic rotation profile measurement (CXRS+DNBI)

► Plasma shape **designed** to maximise the asymmetry effect

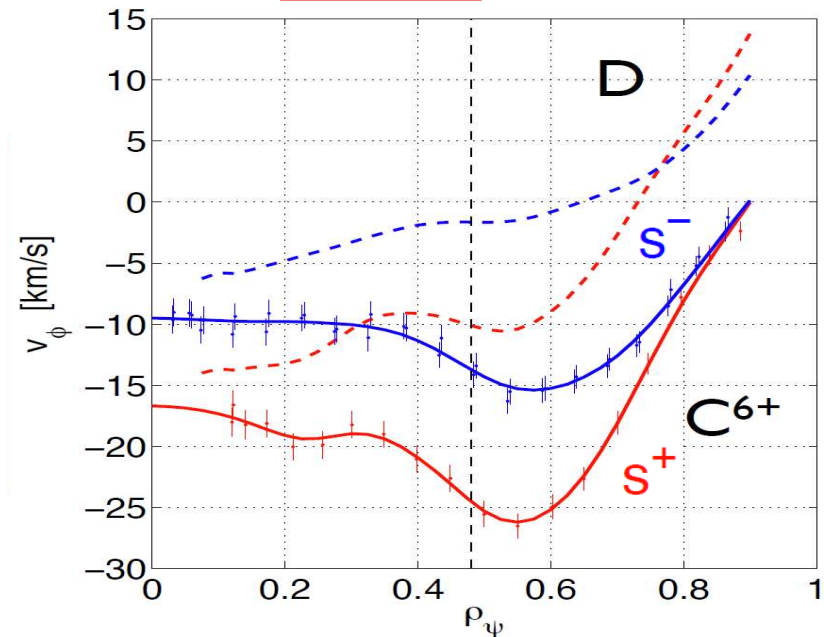
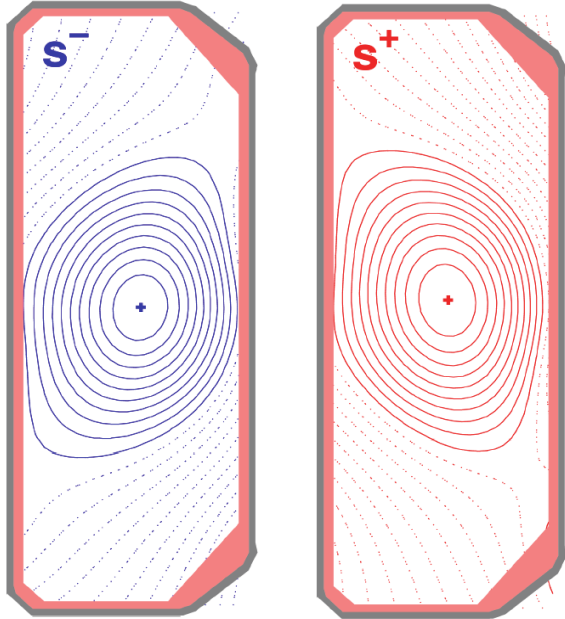
Validated by experiments in TCV

[Camenen PRL 10, PPCF 10]



► **Theory** : up-down asymmetry → residual stress [Camenen PRL09, PoP09]

$$-R_0 \frac{\partial \omega_\varphi}{\partial r} = -\frac{R_0 V_{co}}{\chi_\varphi} \omega_\varphi - \frac{C_{\text{other}}}{\chi_\varphi} - \frac{C_{\text{FS}}}{\chi_\varphi}$$



► As predicted, gradient smaller for the s- shape compared to the s+ shape

► Agreement with predictions also in all the other combinations b+/- & j+/-

The symmetry breaking by a finite average radial wave number



$$\frac{\Pi_\phi}{nmR} = -\chi_{\phi\parallel} R \frac{\partial \omega_\phi}{\partial r} + \left(V_\phi + \frac{\Gamma_n}{n} \right) R \omega_\phi + \frac{\Pi_{FS}}{nmR} + \boxed{M_\parallel \gamma_E + \rho_*^\alpha \frac{\Pi_*}{nmR}}$$

Parallel velocity shear
 [Mattor PF 88, Peeters PoP 05]

Pinch
 [Peeters PRL 07, Hahn PoP 07, Waltz PoP 07]

Particle flux

Up-down asymmetry
 [Camenen PRL 09]

ExB shearing
 [Dominguez PFB 93, Garbet PoP 02, Gurcan PoP 07, Waltz PoP 09, Casson PoP 09]

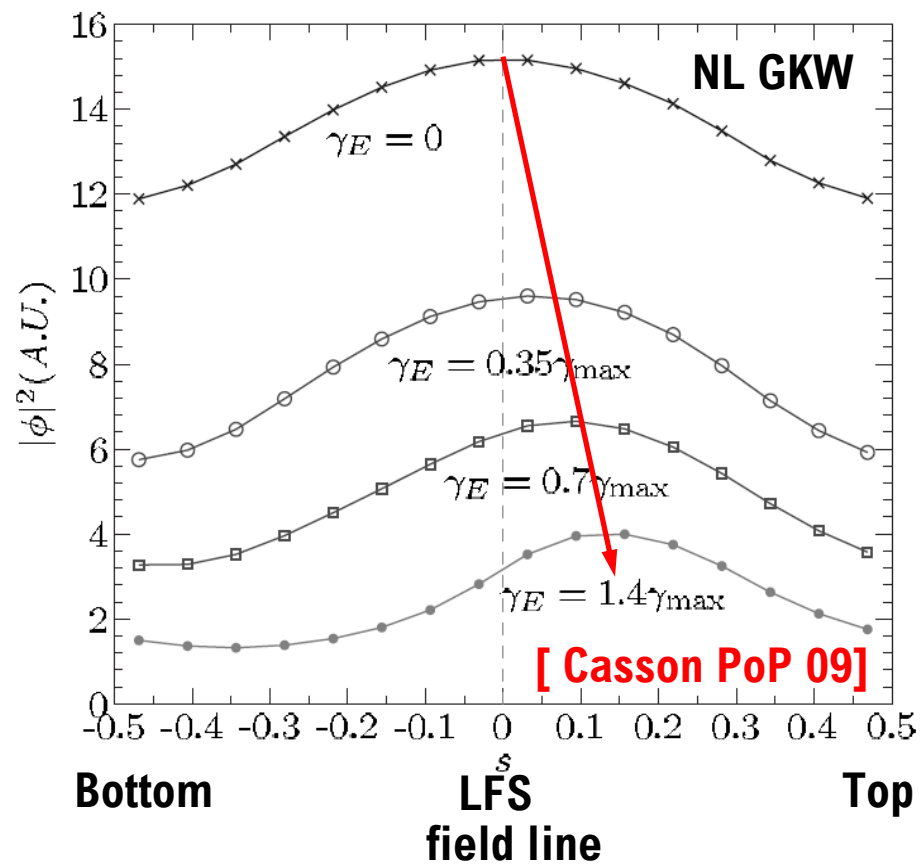
Finite ρ^*

➤ Symmetry breaking by finite average radial wave number $\langle k_r \rangle$

ExB shear, Mechanism

$$\frac{\Pi_\phi}{nmR} = -\chi_{\phi\parallel} R \frac{\partial \omega_\phi}{\partial r} + \left(V_\phi + \frac{\Gamma_n}{n} \right) R \omega_\phi + \frac{\Pi_{FS}}{nmR} + \boxed{M_\parallel \gamma_E} + \rho_*^\alpha \frac{\Pi_*}{nmR}$$

- Maximum of the radially averaged electrostatic potential displaced from the LFS midplane
- Leads to a finite $\langle k_r \rangle$
[Staebler NF 91, Dominguez PFB 93]
- Finite $\langle k_r \rangle$ produces finite momentum flux which, in simple linearized model for small perturbations can be assumed to increase linearly with γ_E
- Actual situation more complex and requires nonlinear simulations



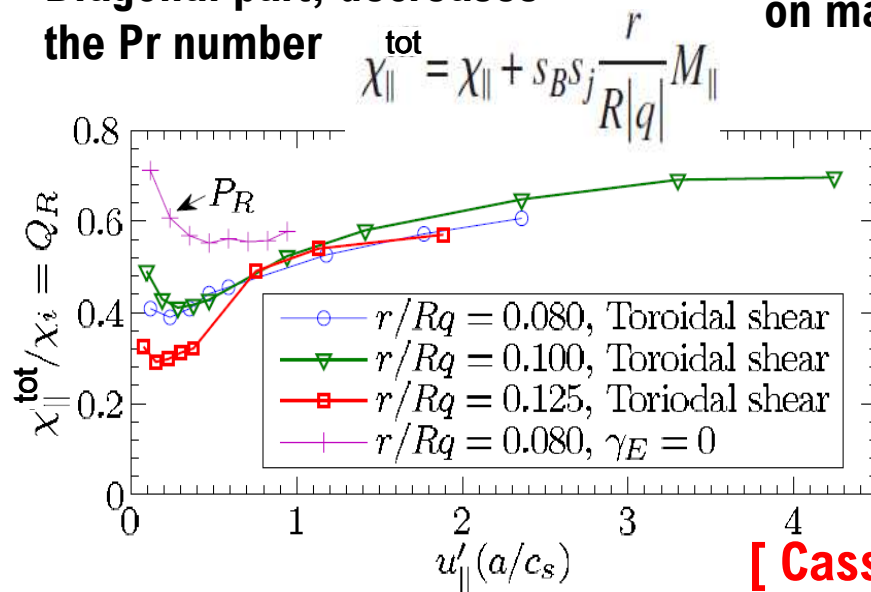
ExB shear, diagonal and off-diagonal components

$$\mathbf{E} = \frac{\nabla p}{en} - \mathbf{V} \times \mathbf{B}$$

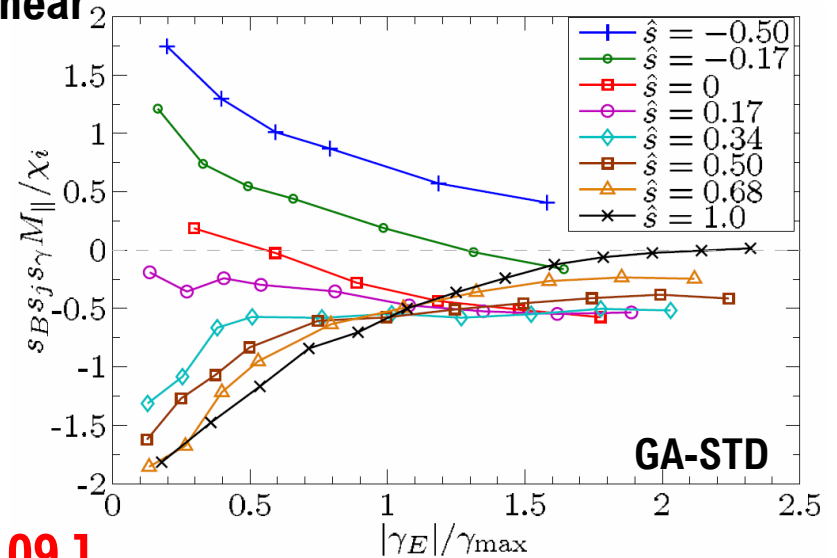
$$\frac{\Pi_\phi}{nmR} = -\chi_{\phi\parallel} R \frac{\partial \omega_\phi}{\partial r} + \left(V_\phi + \frac{\Gamma_n}{n} \right) R \omega_\phi + \frac{\Pi_{FS}}{nmR} + \boxed{M_\parallel \gamma_E} + \rho_*^\alpha \frac{\Pi_*}{nmR}$$

$$\gamma_E \approx \frac{\epsilon}{q} \frac{R^2}{v_{th}} \frac{d\omega_\phi}{dx} + \frac{\rho_*}{2} \left[\frac{R}{L_T L_N} - \left(\frac{R}{L_N} \right)^2 + \frac{R^2}{n} \frac{d^2 n}{dr^2} + (1 - k_{neo}) \frac{R^2}{T} \frac{d^2 T}{dr^2} \right]$$

Diagonal part, decreases the Pr number



Residual stress, nonlinear dependence, sign depends on magnetic shear

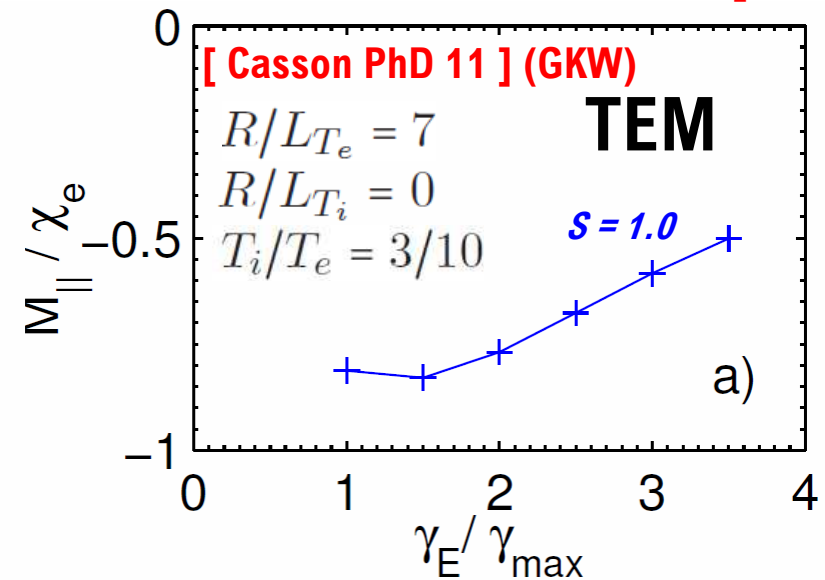
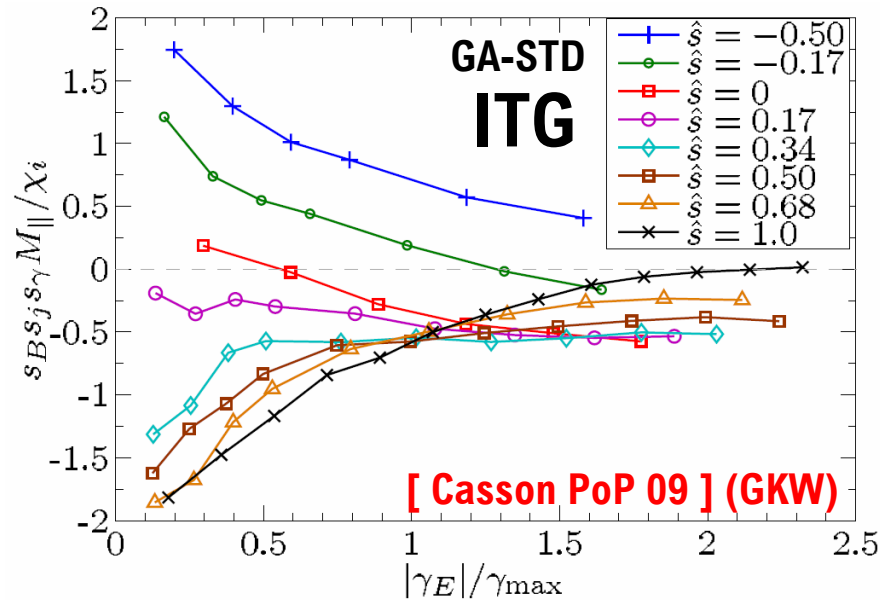


[Casson PoP 09]

ExB shear residual stress changes sign with sign of γ_E , current & field, but not with turbulence propagation



- ITG and TEM produce residual stress in the same direction [Waltz PoP 11 Casson PhD 11]



- Impact of ExB shearing on momentum transport included also in TGLF (of interest for applications in STs) [Staebler PoP 11]
- In contrast to particle transport, all off-diagonal terms of momentum transport described so far do not reverse direction with the direction of propagation of the turbulence

Additional ρ_* effects

$$\frac{\Pi_\phi}{nmR} = -\chi_{\phi\parallel} R \frac{\partial \omega_\phi}{\partial r} + \left(V_\phi + \frac{\Gamma_n}{n} \right) R \omega_\phi + \frac{\Pi_{FS}}{nmR} + M_\parallel \gamma_E + \boxed{\rho_*^\alpha \frac{\Pi_*}{nmR}}$$

➤ So far local limit, lowest order ρ_*

➤ At higher order no symmetry, many effects possible

[e.g. Diamond PoP 08, McDevitt PRL 09, McDevitt PoP 09, Gurcan PoP 10, Parra PoP 10, Camenen PoP 11, Waltz PoP 11, ...]

Additional ρ_* effects

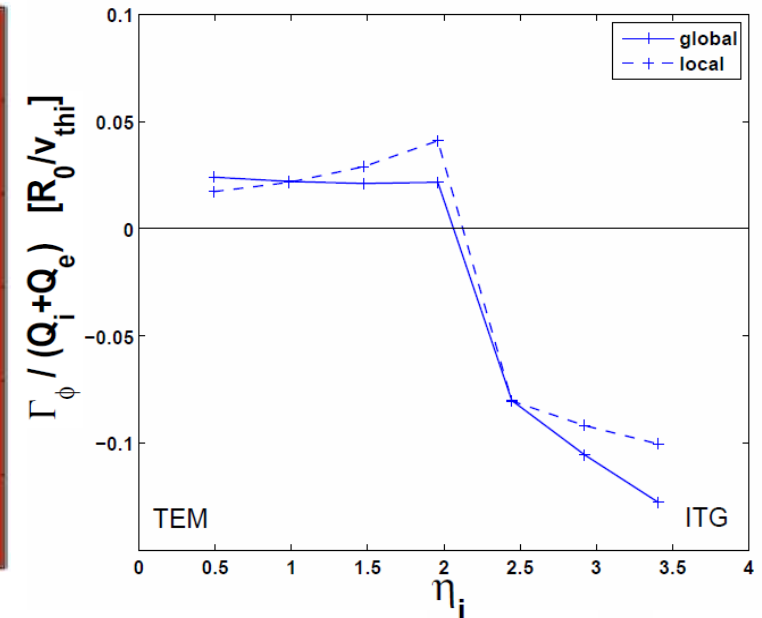
$$\frac{\Pi_\phi}{nmR} = -\chi_{\phi\parallel} R \frac{\partial \omega_\phi}{\partial r} + \left(V_\phi + \frac{\Gamma_n}{n} \right) R \omega_\phi + \frac{\Pi_{FS}}{nmR} + M_\parallel \gamma_E + \boxed{\rho_*^\alpha \frac{\Pi_*}{nmR}}$$

- **So far local limit, lowest order ρ_***
- **At higher order no symmetry, many effects possible**
 [e.g. Diamond PoP 08, McDevitt PRL 09, McDevitt PoP 09, Gurcan PoP 10, Parra PoP 10, Camenen PoP 11, Waltz PoP 11, ...]
- **Which are the dominant effects, and under which conditions ?**
- **Two parallel ways to proceed**
 - 1. Theoretical assessment** of the scaling of each mechanism versus ρ_*
 - 2. Experimental investigation** of properties of residual stress (intrinsic rotation) and identify mechanisms in the theory which have the same properties, parametric dependences, relationship with turbulence type
- **Phenomenology of intrinsic rotation reversals of particular interest (connection with LOC-SOC transitions suggests relationship with turbulence type)**
 [Rice NF 2011, McDermott PPCF 2011, Angioni PRL 2011, Rice PRL 2011]

Profile shearing gives example of residual stress which reverses direction with turbulence propagation



[Camenen NF 11, Waltz PoP 11, radial variation of turbulence intensity Gurcan PoP 10]



- Radial variation tilts eddies in opposite directions for TEM and ITG (finite θ_0)

- Linear fluid model, single mode
- $$\frac{C^*}{\chi_\phi} = -s_j \left| \frac{\hat{s}}{q} \right| \left(R/L_n + 4 - \frac{4}{q^2} \right) \left[2 \frac{a}{R_0} R/L_{Ti} \rho_* \right]^{\frac{1}{3}}$$

[Camenen NF 11]

- Nonlinear global simulations required to compute real scaling [Global sim : Holod PoP 08 (GTC), Wang PRL 09,11 (GTS), Waltz PoP 11 (GYRO), Abiteboul PoP 11 (GYSELA)]

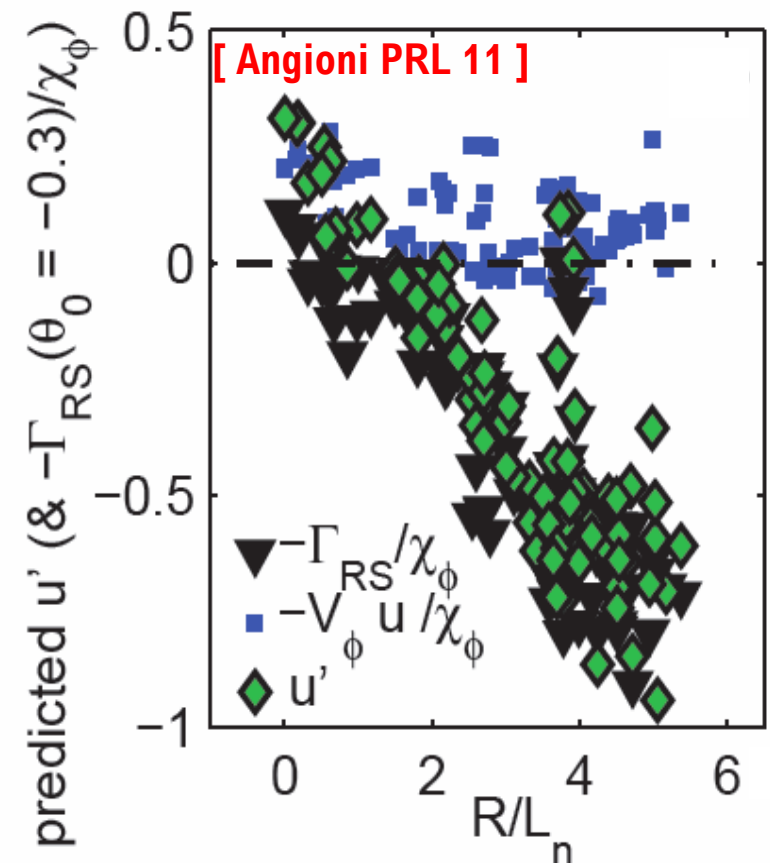
Relation between finite $\langle k_r \rangle$ and residual stress, density gradient dependence



- Assuming a finite θ_0 (due to a given symmetry breaking mechanism), the impact on the strength of the residual stress is connected to R/L_n

[Analytical studies, GK **Diamond PoP 08**, fluid **Camenen PoP 11**]

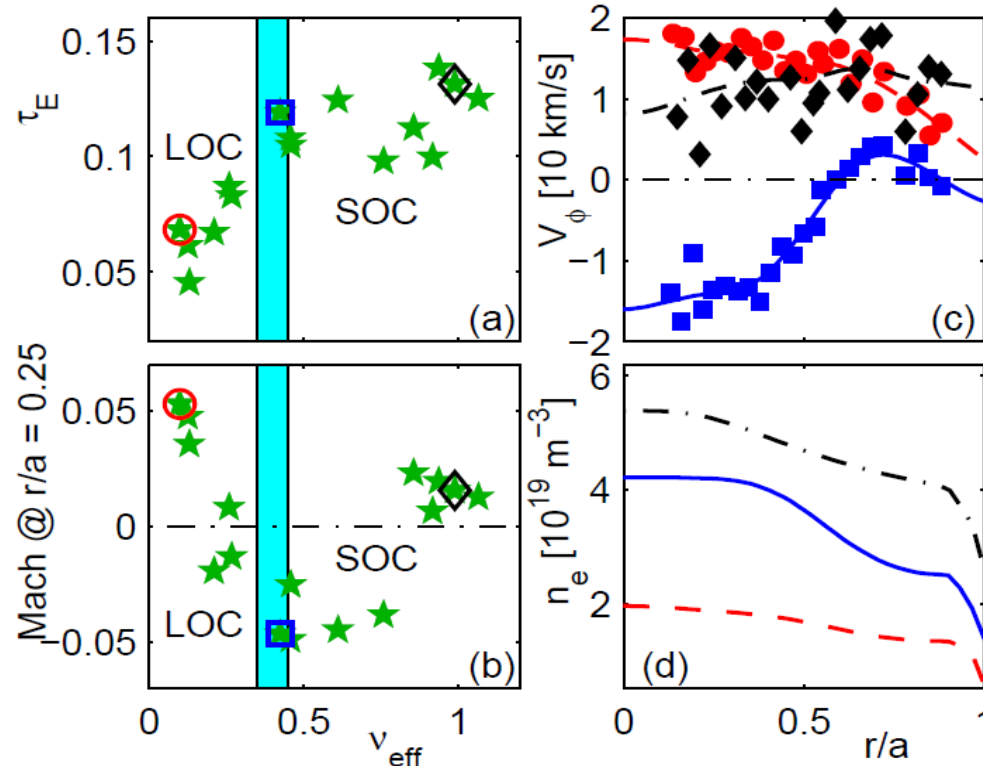
- Consistent with local GK code (GS2) with imposed fixed tilting angle $\theta_0 = -0.3$
- Different symmetry breaking mechanisms produce different relations between tilting angle θ_0 and $\langle k_{||} \rangle$
- From theory standpoint, investigating strength of residual stress by varying different parameters is an important information to interpret the experiment



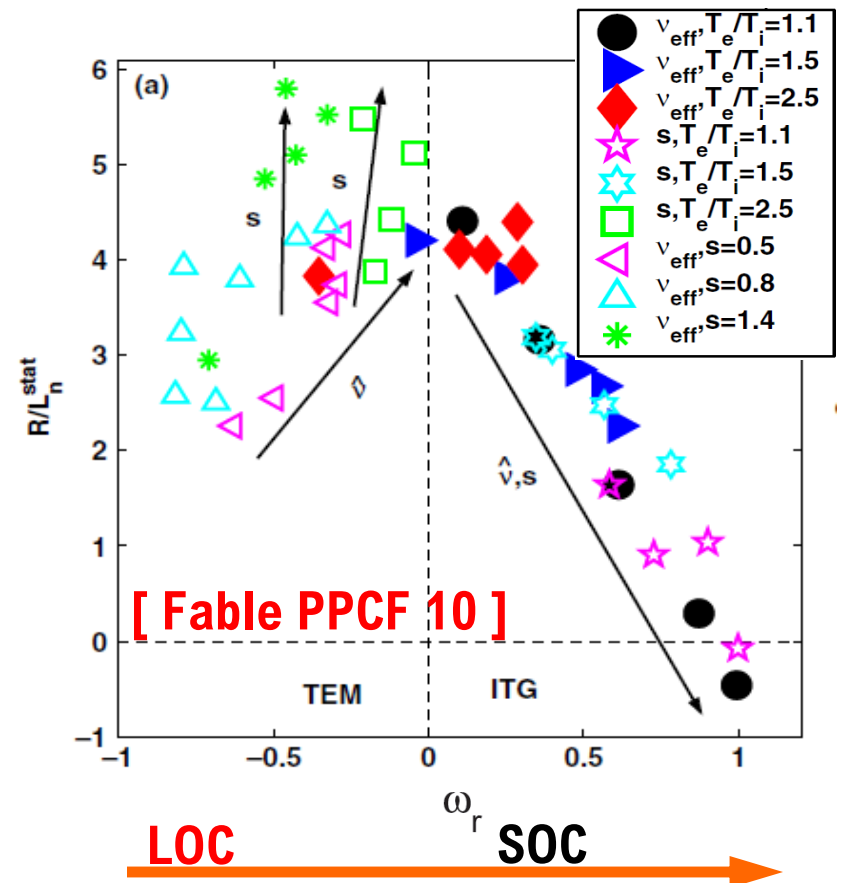
Strength of residual stress producing counter-current rotation & logarithmic density gradient



- Data from a LOC-SOC transition in AUG suggest a connection between strength of RS producing counter-current central rotation and R/L_n



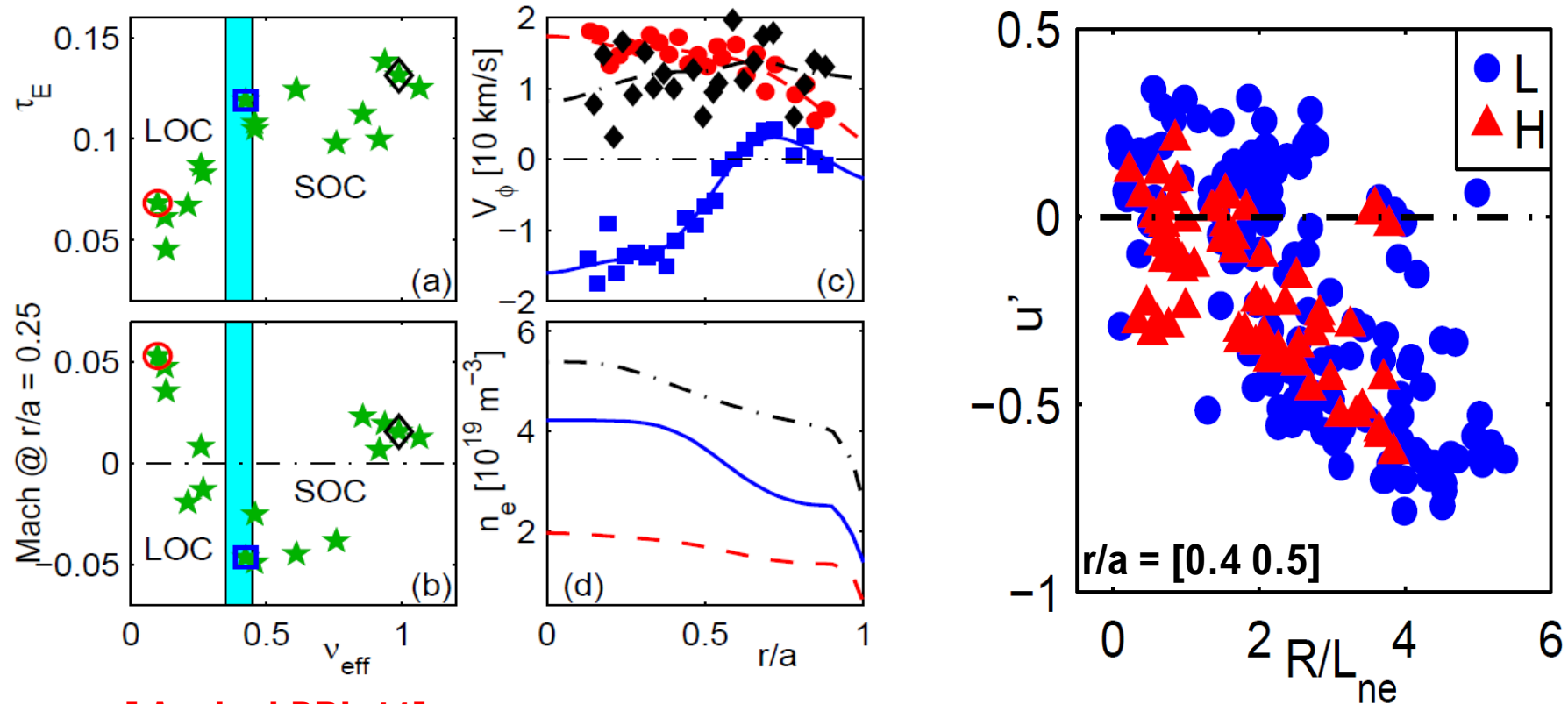
[Angioni PRL 11]



Strength of residual stress producing counter-current rotation & logarithmic density gradient



- Data from a LOC-SOC transition in AUG suggest a connection between strength of RS producing counter-current central rotation and R/L_n
- Confirmed by analysis of large database of L- & H-mode intrinsic rotation profiles

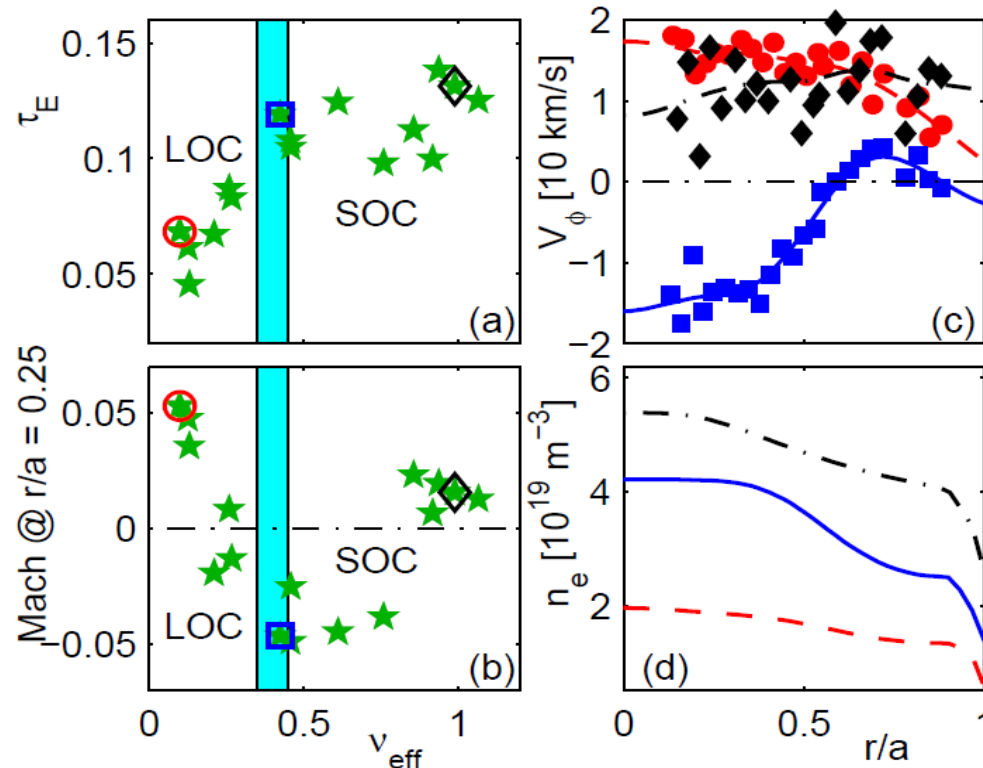


[Angioni PRL 11]

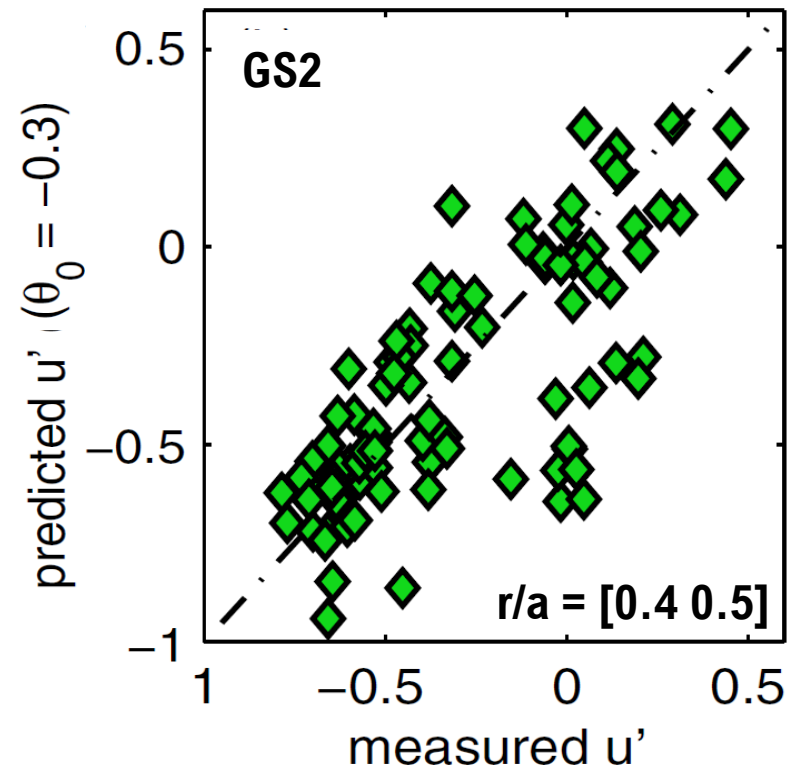
Strength of residual stress producing counter-current rotation & logarithmic density gradient



- Data from a LOC-SOC transition in AUG suggest a connection between strength of RS producing counter-current central rotation and R/L_n
- Confirmed by analysis of large database of L- & H-mode intrinsic rotation profiles



[Angioni PRL 11]



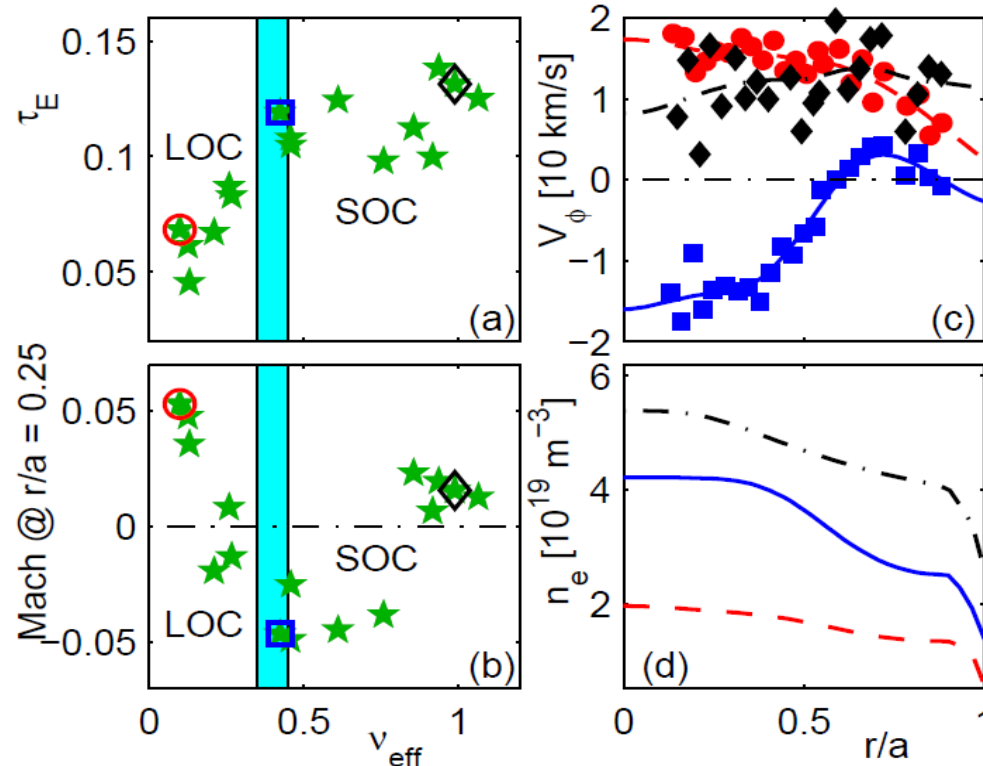
Well predicted imposing a fixed tilting angle in linear GK (-0.3 rad for TEM subset)

Strength of residual stress producing counter-current rotation & logarithmic density gradient

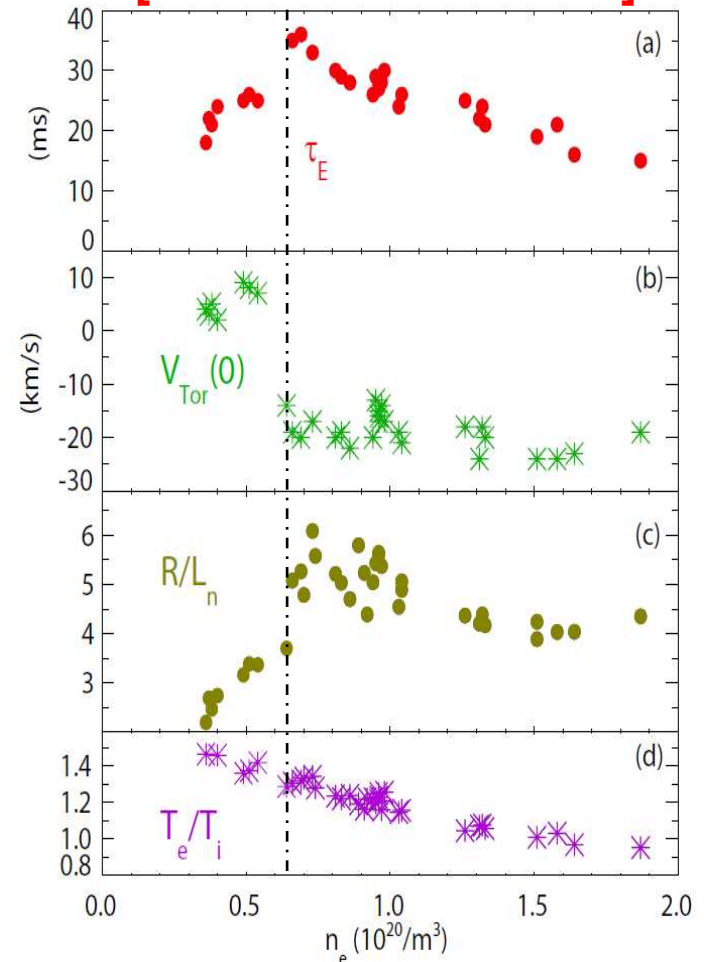


- Data from a LOC-SOC transition in AUG suggest a connection between strength of RS producing counter-current central rotation and R/L_n
- Not inconsistent with C-Mod results

[Rice NF 11 & PRL 11b]



[Angioni PRL 11]



General conclusions

- Transport of particle & toroidal momentum present **extremely interesting physics**, because of **existence & relevance of non-diffusive terms**
- These are **predicted theoretically and have been identified experimentally**
- Non-diffusive terms strongly impact shapes of density & toroidal rotation profiles, and play essential role on confinement, stability, & ultimately fusion performance
- There are **evidences of (theoretically predicted) connections between these two channels**, in the strength of the momentum pinch and of the residual stress, and in the role of rotation on impurity transport
- Appropriate (quantitative) predictions of these non-diffusive terms require rather **involved (consistent) models** (simple formulae not suited for exp. comparisons)
- Particularly in momentum transport, **these terms are inter-dependent** through the average parallel wave number (comprehensive and consistent models required)
- For both channels, most critical questions are on the behaviour at the **boundary**

THE END

Observations of intrinsic rotation and rotation reversals connected with physics of residual stress

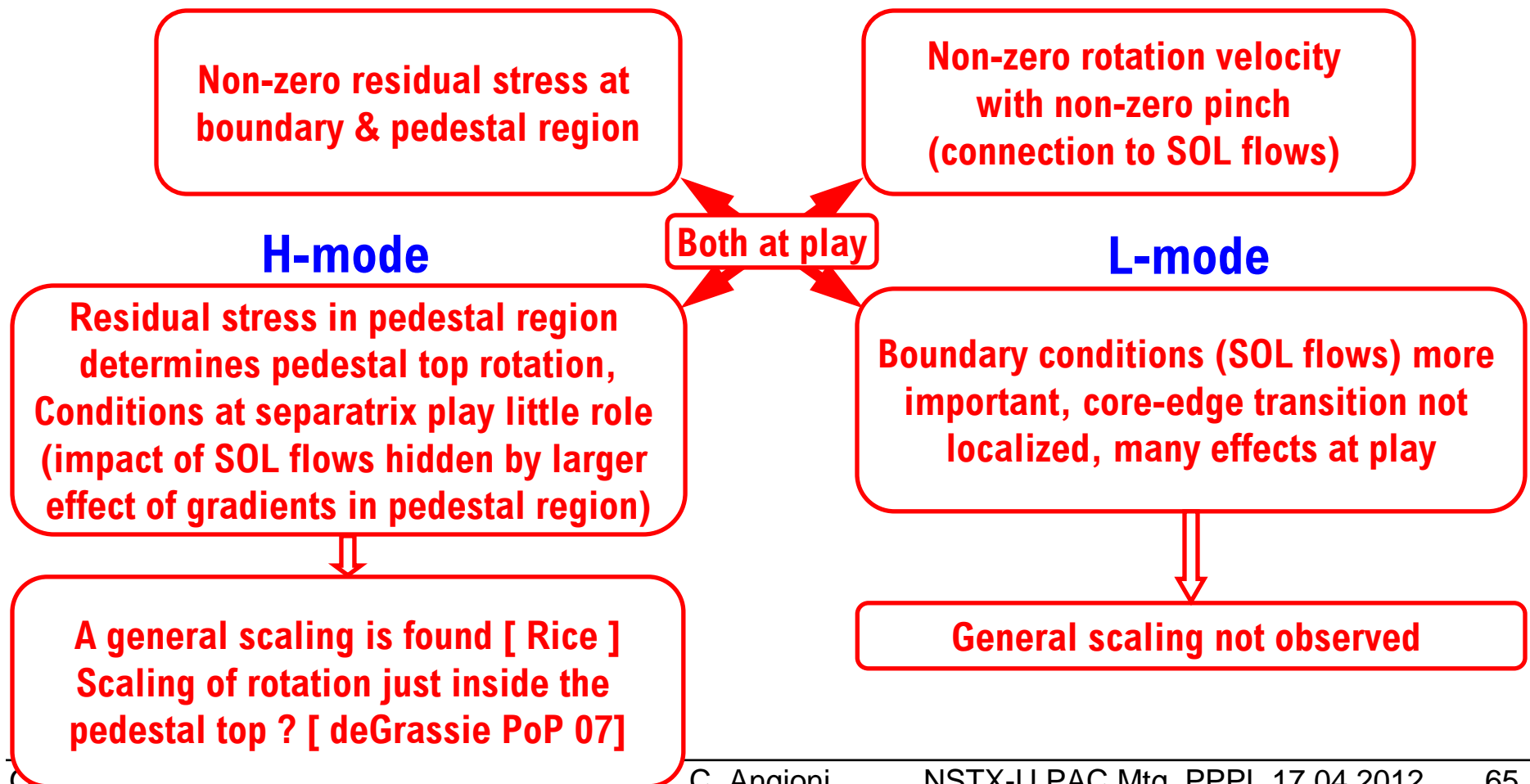


- Profile shape can vary and cross zero (signature of residual stress effect)
- Rotation at least in H-mode appears to follow a general scaling [Rice NF 07, deGrassie PoP 07] (is Rice scaling to be applied to central or to pedestal-top rotation ?)
- At the edge role of temperature gradient in driving intrinsic rotation pointed out in experiments [deGrassie PoP 09, Rice PRL 11a] and theory [Stoltzfus-Dueck PRL 11]
- In the core, connection of reversals with LOC-SOC transitions suggests at least partly a relationship with turbulence type [Rice NF 11, Angioni PRL 11, Rice PRL 11b]
- In the core, correlation between intrinsic toroidal rotation and electron density gradients pointed out recently in AUG [McDermott EPS & PPCF 11, Angioni PRL 11]
- Suggests that core turbulence transitions impact (at least partly) the RS, but also the density profile and, as by-product, also the strength of the RS

Momentum transport at the edge, generality of Rice scaling, where and when ?

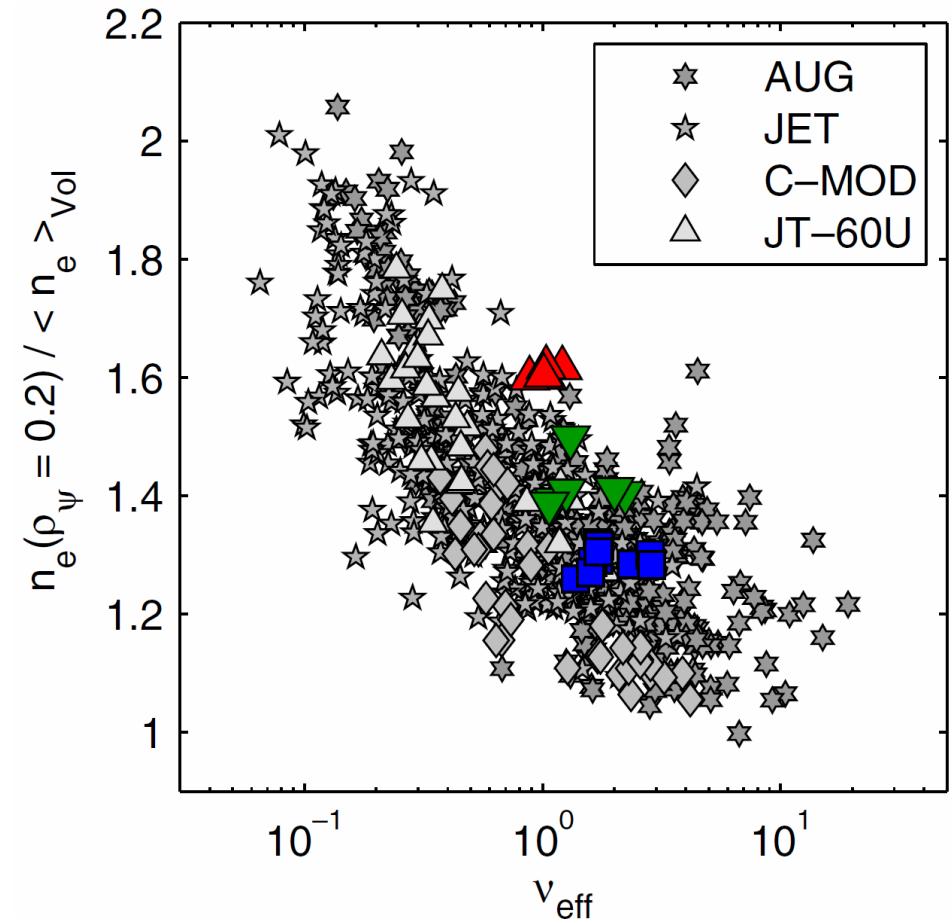
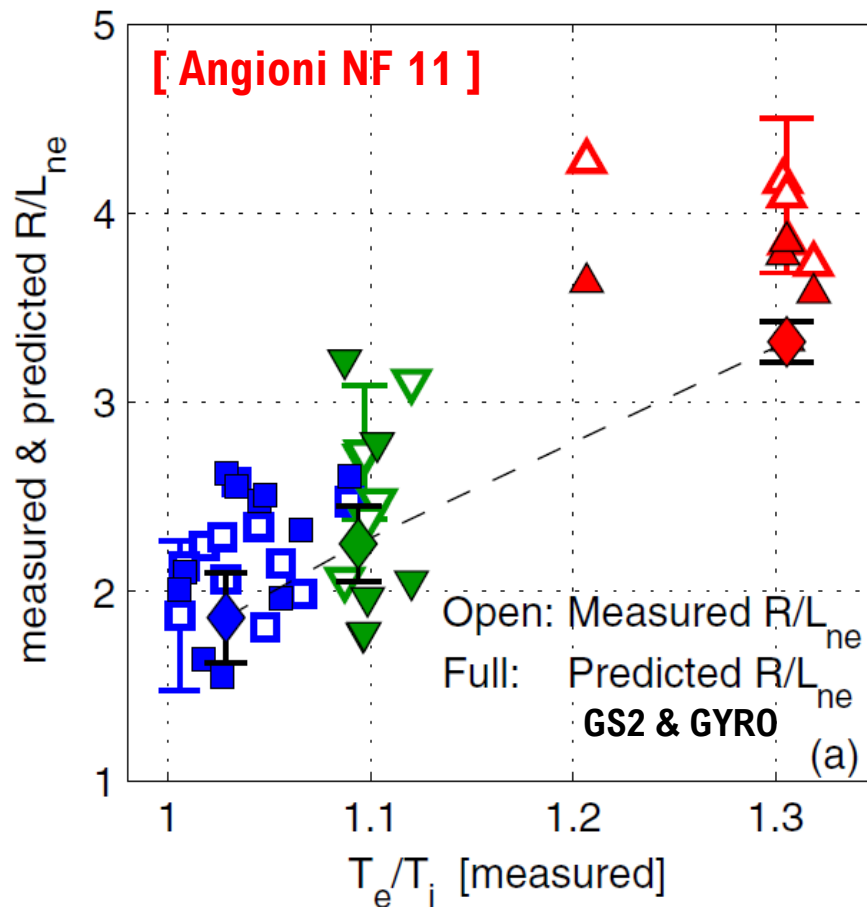


- Residual stresses are measured (and predicted) to be particularly large at the edge (ExB shearing, other ρ^* effects, up-down asymmetry, orbit effects, ...)
- A picture for discussion [suggested (at least to me) by Diamond NF 09]



Usual back-up slides on particle transport (from last ITPA Mtg)

Experiment and theory consistently show increase of peaking with increasing T_e/T_i in ITG turbulence

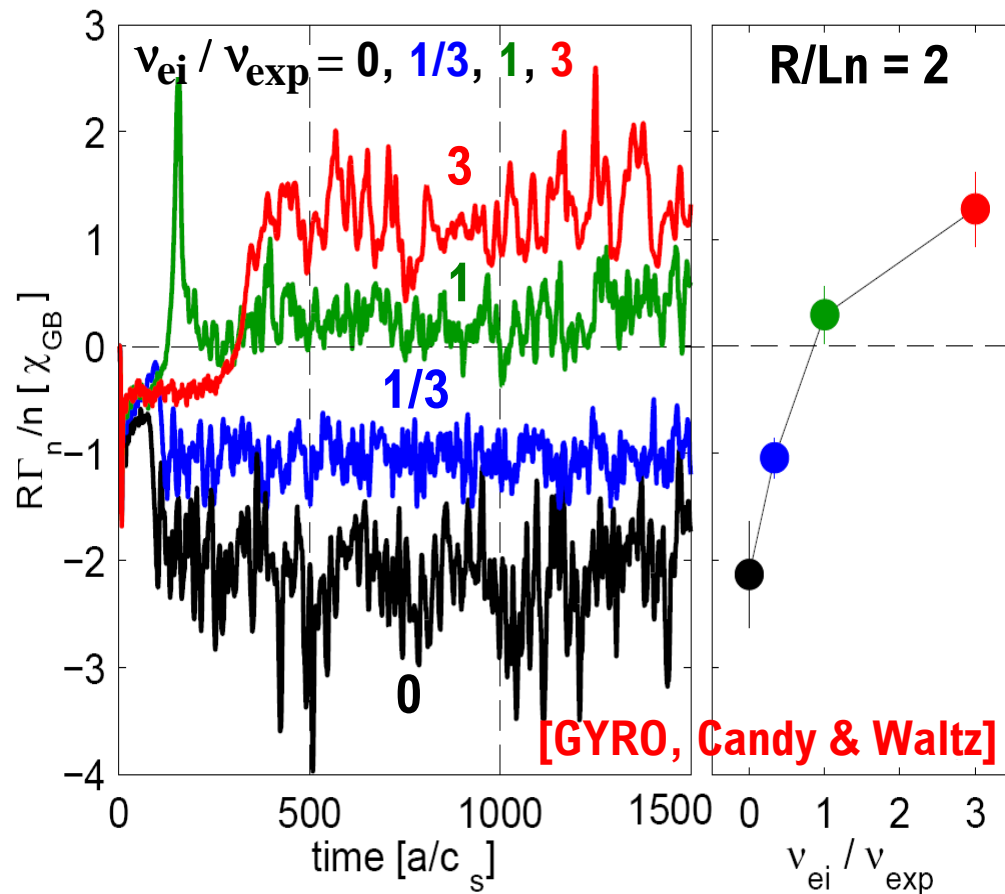


- Explains (& predicts) why central ECH increases density peaking with ITG modes
- Increase of L_{Ti}/L_{Te} , T_e/T_i and drop of collision frequency reduce mode frequency & increase peaking

Collisions strongly affect turbulent convection, outward (inward) contribution for ITG (TEM) modes



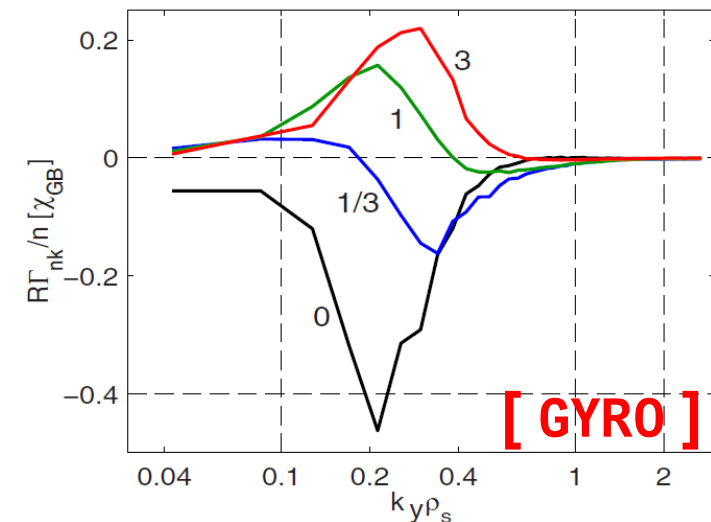
[Angioni PoP 09, nonlinear gyrokinetic simulations, ASDEX Upgrade parameters at ITER collisionality]



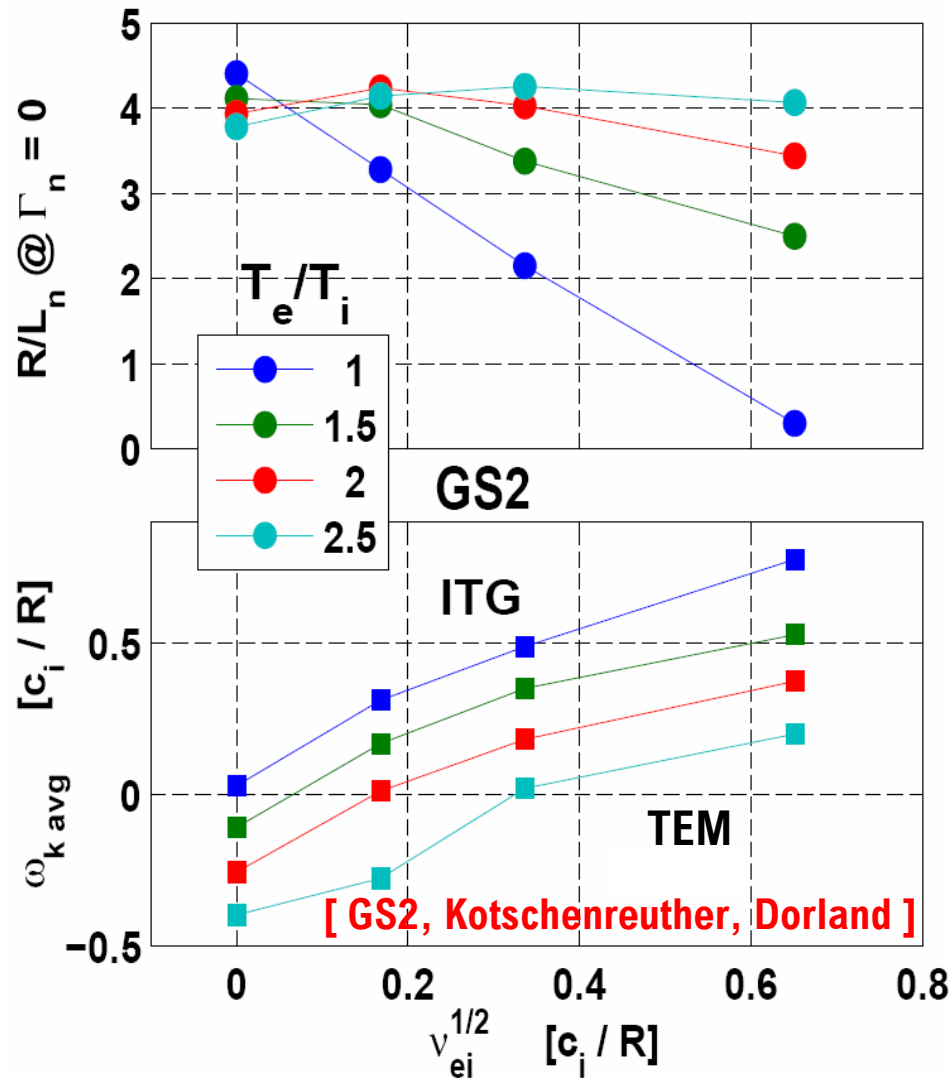
- With ITG modes, increase of collisionality produces a reduction of inward convection
[Angioni PRL 03, with fluid GLF23, Estrada-Mila PoP 05, GYRO]

- Collisional contribution related to type of instability, ITG outward, TEM inward

[Angioni PoP 09, Fable PPCF 10]

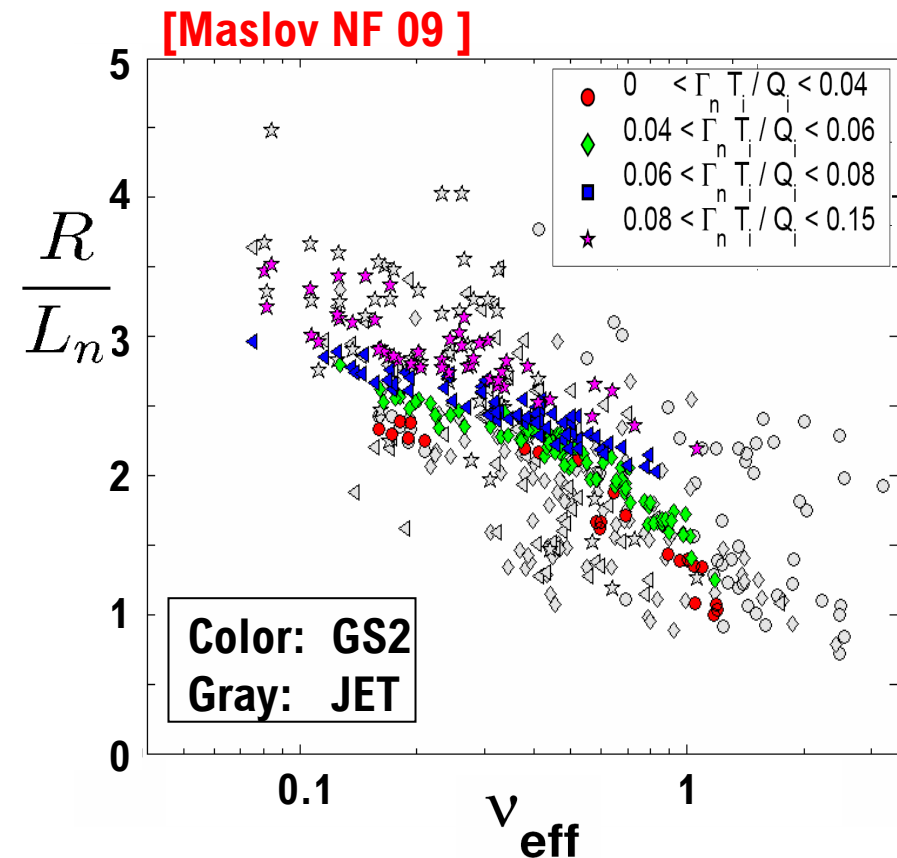
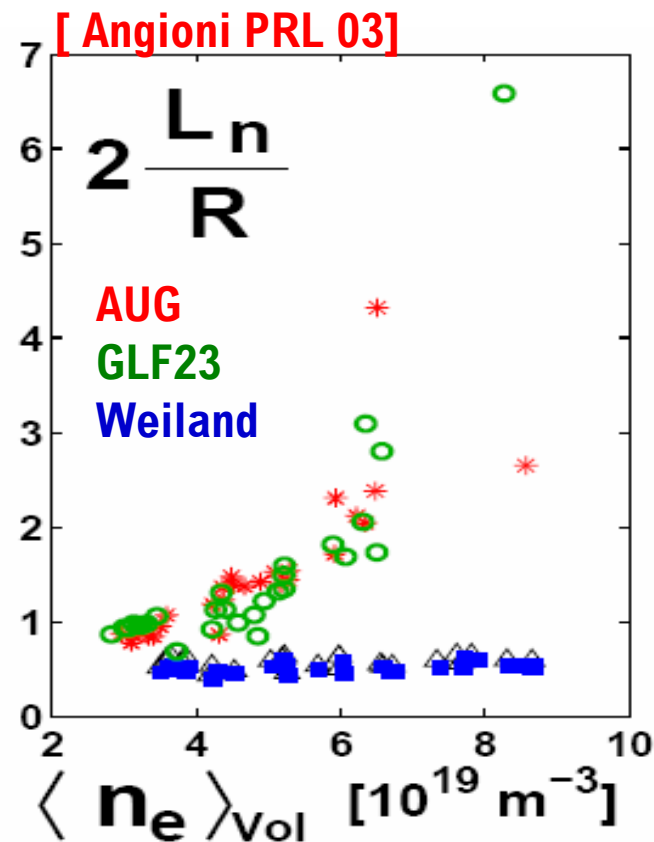


Collisions strongly affect turbulent convection, outward (inward) contribution for ITG (TEM) modes



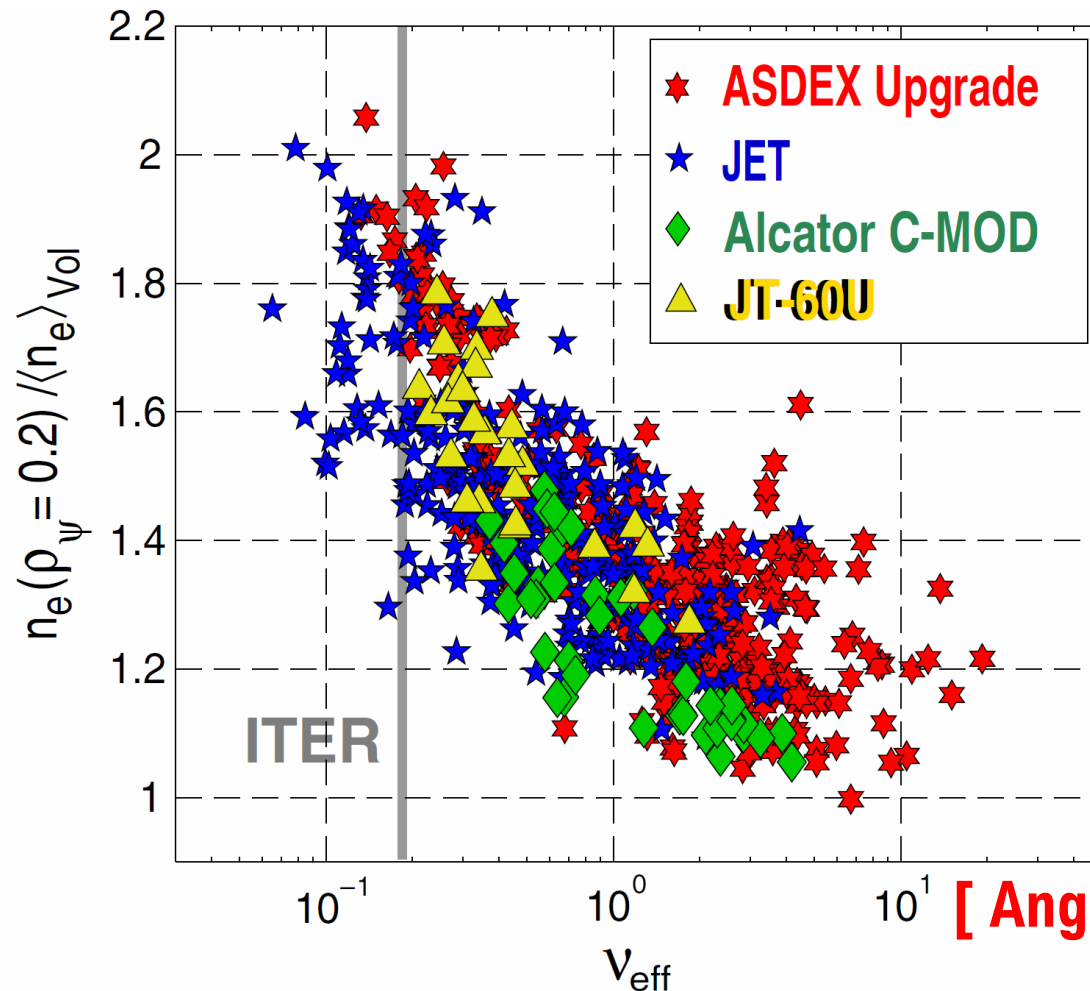
- With ITG modes, increase of collisionality produces a reduction of inward convection
[Angioni PRL 03, with fluid GLF23, Estrada-Mila PoP 05, GYRO]
- Collisional contribution related to type of instability, ITG outward, TEM inward
[Angioni PoP 09, Fable PPCF 10]
- Density peaking predicted to decrease with increasing collisionality in ITG, to weakly increase (almost unaffected) in TEM

Observations in H-mode plasmas agree quantitatively with theory predictions on role of collisions in ITG turbulence



- Collisionality dependence identified through transport modelling comparing predictions of models with and without collisions [Angioni PRL and PoP 03]
- Quantitative agreement between GS2 gyrokinetic quasi-linear calculations and JET data, evaluation of impact of NBI source from theory [Maslov NF 09]

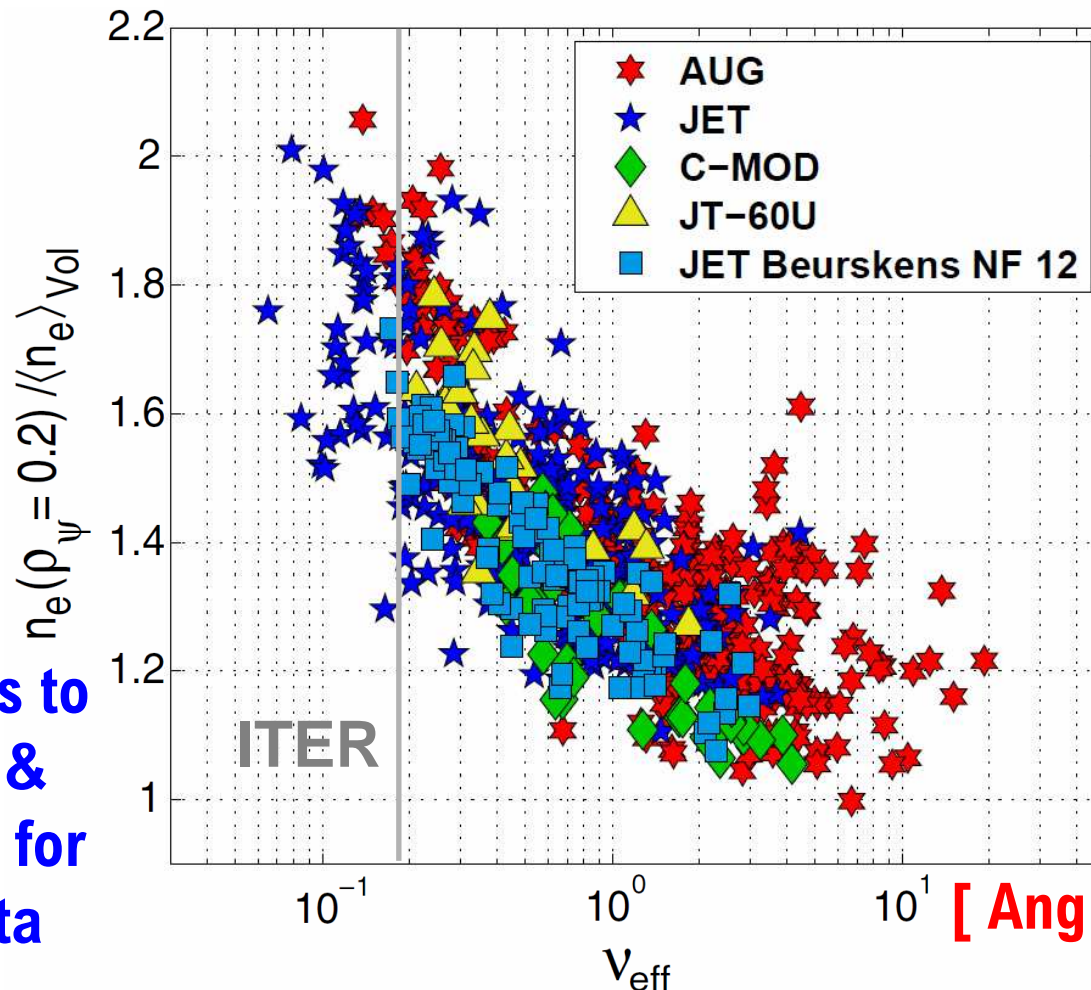
Density peaking in AUG, C-MOD, JET, JT-60U follows the same dependence vs collisionality



[Angioni PPCF 09]

- AUG [Angioni PRL 03], JET [Weisen NF 05], C-Mod [Greenwald NF 07], JT-60U [Takenaga NF 08]

Density peaking in AUG, C-MOD, JET, JT-60U follows the same dependence vs collisionality



Special thanks to
L. Frassinetti &
M. Beurskens for
recent JET data

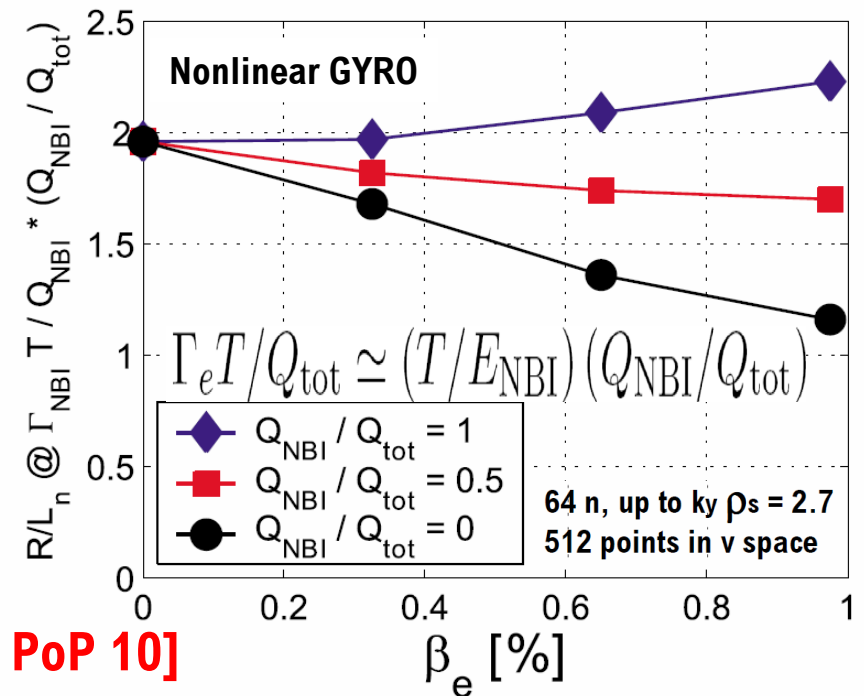
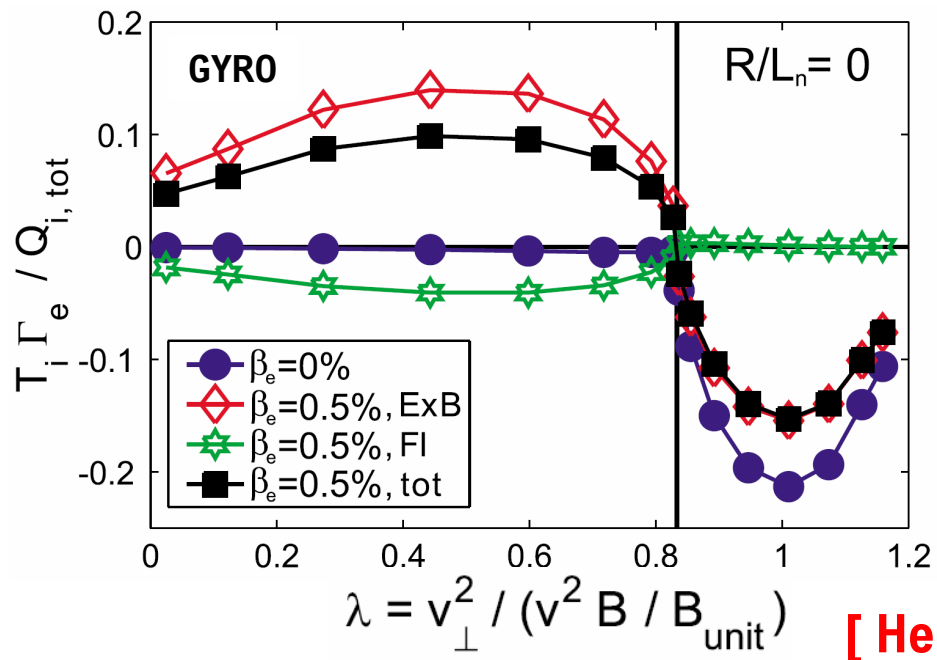
[Angioni PPCF 09]

➤ AUG [Angioni PRL 03], JET [Weisen NF 05], C-Mod [Greenwald NF 07], JT-60U [Takenaga NF 08], JET [Beurskens NF submitted]

Theoretical predictions of electromagnetic effects, towards the prediction of the density profile in high β scenarios



- Electromagnetic effects imply a non-adiabatic response of passing electrons
- Passing electrons are transported outward by convection



- High β predicted to lead to a significant reduction of density peaking in the absence of central fuelling
- This should motivate studies of density profiles in low collisionality high β_e plasmas with and without NBI heating (relevant also for DEMO scenarios)